

Theory of ballistic-hydrodynamic phase transition in flow of two-dimensional electrons

A. N. Afanasiev, P. S. Alekseev, A. A. Greshnov, and M. A. Semina
Ioffe Institute, Politekhnicheskaya 26, 194021 St. Petersburg, Russia

Phase transitions are characterized by a pronounced change in the type of dynamics of microparticles, and their description usually requires quantum statistics. Recently, a peculiar type of conductors was discovered in which two-dimensional (2D) electrons form a viscous fluid. Here we reveal and study a novel type of phase transitions in such systems between the ballistic and the hydrodynamic flows of classical 2D electrons. We theoretically trace an emergence of a fluid phase of interacting hydrodynamic electrons from a “dust” of ballistic electrons with an increase of magnetic field. This transition manifests itself by a sharp kink in the dependence of the longitudinal and the Hall resistances on magnetic field, reflecting the switching of the type of the particle dynamics. Our analysis shows that such transition was observed in recent experiments on 2D electron hydrodynamics in graphene and high-mobility GaAs quantum wells. The effect is not only of scientific interest providing a simple mechanism of formation of a fluid phase from individual particles, but may be useful for diagnostics of novel microstructures for future devices based on hydrodynamic electrons.

1. Introduction. Frequent collisions between electrons in high-quality conductors at low temperatures can lead to formation of a viscous electron fluid and the realization of the hydrodynamic regime of charge transport. Although the theory of such fluid has been actively developed for a very long time [1],[2], the formation of the viscous flow of an electron fluid was experimentally demonstrated only recently in high-quality graphene, Weyl semimetals, and GaAs quantum wells [3]-[23]. The hydrodynamic flow in these experiments was detected by a specific dependence of the mean sample resistivity on the sample width [3]; by observation of the negative nonlocal resistance [4, 5, 17], the giant negative magnetoresistance [10–16, 18, 19], and the huge magnetic resonance at twice cyclotron frequency [20–23].

Much attention was paid to the transition between the ballistic and the hydrodynamic regimes of electron transport. In Ref. [8] and [9] measurements of profiles of the Hall electric field and the current density of 2D electron flow in graphene stripes made it possible to observe this transition at low temperatures with increase of magnetic field. In those works a peculiar nonmonotonic magnetoresistance in the both regimes was also observed. Similar magnetoresistance was detected in long samples of high-quality GaAs quantum wells [16, 18], that, apparently, evidences the realization of the ballistic-hydrodynamic transition also in the last systems.

A qualitative theory of the ballistic-hydrodynamic transition of 2D electron flow in the absence of magnetic field was constructed in Ref. [24] for a sample containing macroscopic round obstacles. It was shown that the ballistic-hydrodynamic transition in this system, occurring with changing the interparticle scattering rate, has the character of a smooth crossover.

A numerical theory of the ballistic-hydrodynamic transition for 2D electrons in stripes in a perpendicular magnetic field was developed in Ref. [25]. The obtained longitudinal and the Hall resistances as functions of magnetic field exhibit kinks at the critical magnetic field $B = B_c$

above which the diameter of the electron cyclotron orbit $2R_c$ becomes smaller than with the sample width W and a hydrodynamic flow begins to form. In Ref. [26], a Poiseuille flow of 2D electrons in magnetic field was theoretically studied in more details. In particular, the profiles of the Hall electric field over the sample cross section were calculated below and above the transition point, $B = B_c$, and an analytical solution of the kinetic equation was constructed for the ballistic regime at $B < B_c$. It was shown that an increase of the curvature of the Hall electric field takes place with the transition from ballistic to the hydrodynamic regimes.

Here we develop a simple analytical theory of the ballistic-hydrodynamic transition and the ballistic transport for 2D interacting electrons in a perpendicular magnetic field. We reveal that the transition between the ballistic and the hydrodynamic regimes of transport with increase of the magnetic field is a sharp phase transition for narrow high-quality stripes. The electron dynamics, although being qualitatively changed when the magnetic field B crosses the critical field B_c , is nevertheless controlled by the electron-electron scattering in both the ballistic, $0 < B_c - B \ll B_c$, and the hydrodynamic, $0 < B - B_c \ll B_c$, vicinities of the transition point $B = B_c$. In order to describe the phase transition quantitatively, we propose a mean field model based on the simplified classical kinetic equation. We show that the longitudinal and the Hall resistances $\varrho_{xx}(B)$ and $\varrho_{xy}(B)$ exhibit kinks at $B = B_c$. We believe that the studied mechanism of the ballistic-hydrodynamic transition is relevant not only for stripes, but also, for example, for 2D electrons in samples with macroscopic obstacles, previously widely studied [15],[27] without taking into account the hydrodynamic effects.

Our analysis shows that the studied ballistic-hydrodynamic phase transition was observed in recent experiments [8, 9, 18]. The nonmonotonous behavior of magnetoresistance $\varrho_{xx}(B)$ measured in Refs. [8, 9, 18], obtained in numerical theory [25], and qualitatively ex-

plained here can be considered as a characteristic sign of the ballistic-hydrodynamic transition in a 2D electron flow. This effect may be employed for diagnostics of the novel structures for future electronic devices with the hydrodynamic charge transport.

We also provide a qualitative explanation of the result obtained in Refs. [28, 29] that the Hall electric field E_H in the ballistic regime at very low B is equal to one half of its conventional value $E_H^{(0)}$ of macroscopic Ohmic samples almost in the central part of a sample. Here-with, provided the sample edges are straight and rough, the Hall electric field in the edge vicinities becomes abnormally high due to the appearance of the electrons on the skipping near-edge trajectories. This can lead to a abnormally large Hall resistance at low B . The last and the related effects were observed many years ago for 2D electrons in Hall bar samples, but was explained up to now only within numerical modeling [30].

2. Ballistic regime. We consider a flow of two-dimensional electrons in a long sample with rough edges (see Fig. 1). Electrons are diffusively scattered on the sample edges that leads to momentum relaxation. In the bulk of the sample, electrons collide one with another conserving their total momentum. We assume that the rate γ of the electron-electron scattering is weak: $W \ll l$, where $l = v_F/\gamma$ is the mean free path and v_F is the Fermi velocity.

At $B < B_c$, when the diameter of the cyclotron circle is larger than the sample width, $2R_c > W$, each electron is predominantly scattered on the edges [see Figs. 1(a,b)]. Therefore the transport at such B is ballistic, and the role of interparticle collisions consists in limitation of the time that electrons spend on the ballistic trajectories. The solution of the kinetic equation [31] shows that the ballistic regime has a fine structure, namely, it is divided into three subregimes. The transition between them is accompanied by the evolution of the current density $j(y)$ and the Hall electric field $E_H(y)$ [see Fig. 2(a-d)] as well as by a nonmonotonic behavior of the longitudinal $\varrho_{xx}(B)$ and the Hall resistances $\varrho_{xy}(B)$ [see Fig. 3].

In the first ballistic subregime, $R_c \gg l^2/W$, the electron trajectories are almost straight. Corrections from the electric and the magnetic fields are small for the electrons those after scattering on an edge, reaches another one or scatter in the bulk. In the limit $\omega_c \rightarrow 0$ all electron except the very vicinities of the stripe edges are of such type [31]. The current density in the bulk region, j , is determined by the mean free path, calculated by averaging of the lengths $l_b^{(1)}(\varphi) = W/\cos\varphi$ of such trajectories over the angle φ between the electron velocity and the normal to the edges [see Fig. 1(a)]. The main contribution to the current comes from the trajectories whose directions are close to the sample edge, $|\pi/2 - |\varphi|| \lesssim W/l$ [28]. Calculation leads to the result $j = (2j_0/\pi) \ln[1/(\gamma W)]$ for the current density in the bulk (here $j_0 = nE_0W/m$).

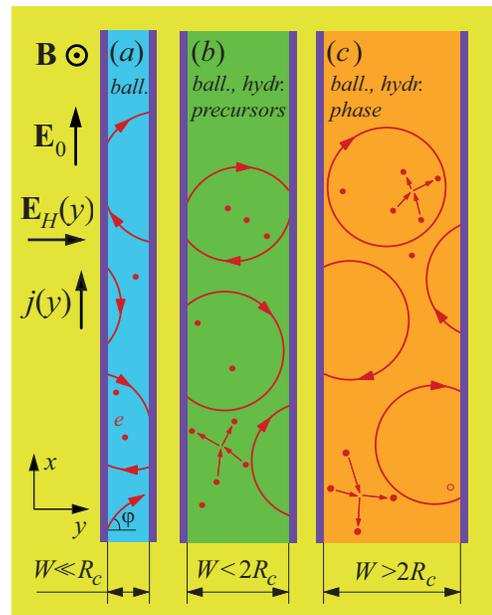


FIG. 1: Two-dimensional electrons in a long sample at low, $W \ll R_c$ (a); intermediate, $W \sim R_c$, $W < 2R_c$ (b); and moderately high, $W \sim R_c$, $W > 2R_c$ (c) magnetic fields. At the critical field B_c corresponding to the condition $2R_c = W$ the ballistic-hydrodynamic phase transition occurs. Above it, $B > B_c$, a group of central electrons appears that do not collide with the edges. In the low vicinity of the transition point, $0 < B_c - B \ll B_c$, electrons on the skipping orbits being close to an almost whole cyclotron rotation provide the main contribution to $j(y)$ and $E_H(y)$.

The magnetic Lorentz force induces a small disturbance on the ballistic trajectories in this subregime. The average length $l_b^{(1)}$ increases due to their small bending by the Lorentz force. This leads the increase of the the mean current j in the bulk of the sample with magnetic field: $j(B) - j(B = 0) \sim B^2$ [28, 31]. The Hall effect in the ballistic regime is related with the requirements of the absence of the velocity and the acceleration of the whole electron ensemble in the y direction. The resulting Hall resistance, $\varrho_{xy} = E_H/j$ in the limit $\omega_c \rightarrow 0$ turns out to be one half of the conventional Hall resistance of macroscopic Ohmic samples [29]:

$$\varrho_{xy} = \frac{1}{2} R_H^0 B, \quad R_H^0 = \frac{1}{n_0 e c}, \quad (1)$$

where n_0 is the equilibrium electron density, e is the electron charge, and c is the velocity of light. In Ref. [29] this result was obtained from solution of the kinetic equation by the perturbation theory by $B \rightarrow 0$. In this work we reveal its physical essence.

Indeed, in the limit $B \rightarrow 0$ and $E_0 \rightarrow 0$ the motion of electrons along the axis x is governed mainly by the electric field E_0 : $v_x(t) = v_F \sin\varphi + E_0 t/m$, where t is the time counted from the last scattering at an edge. Correspondingly, the magnetic Lorentz force linearly depends

on time t : $F_y(t) = eBv_x(t)/c$. The Hall electric field E_H , which compensates this force, is calculated by averaging of $F_y(t)$ over all electrons with any y and φ , using the dependence $t = t(y, \varphi)$ for unperturbed trajectories. As a result, the field E_H acquires an additional factor $1/2$ from averaging of the linear in t term in F_y , as compared with the averaging of the trajectories lengths $l_b^{(1)}(\varphi)$ when calculating the averaged current density j . Such E_H and j lead to result (1) (for details see [31]).

In very vicinities of the sample edges, $W/2 - |y| \lesssim \omega_c/\gamma^2$, an important role is played by the electrons on the skipping trajectories those, after a reflection from an edge, return to the same edge. The length of such trajectories is limited by the closeness of the reflection angle to the sample direction: $l_{b'}^{(1)}(\varphi) \sim R_c|\pi/2 - |\varphi||$ [see Fig. 1(a)]. As a result [31], the Hall field $E_H(y)$ in the near-edge regions becomes abnormally high, of the order of the external field E_0 , and the current density $j(y)$ becomes a nonanalytical function of y and B [see Fig. 2(b)]. Note that such $E_H(y)$ and $j(y)$ in the near-edge regions are calculated by the exact ballistic distribution function which is not a perturbation decomposition by $B \rightarrow 0$ [31]. Correspondingly, the longitudinal and the Hall resistances at the first subregime, $R_c \gg l^2/W$, acquire a peculiar behavior (see Fig. 3).

In real samples, the importance of the contribution of the near-regions $W/2 - |y| \lesssim \omega_c/\gamma^2$, apparently, depends on the sample geometry. For high-quality long stripes with straight edges the contribution from the near-edge flow dominates in magnetoresistance and the Hall effect [31]. For more irregular sample shapes, when the cyclotron radius is larger than the radius of curvature of the edge profiles, the described above near-edge regions are not formed and the bulk contribution to the Hall effect and the magnetoresistance may dominate (see Fig. 3).

In the second ballistic subregime, $W \ll R_c \ll l^2/W$, electron paths become more bent [see Fig. 1(b)]. Their maximal length is now limited by geometry in the whole sample and is estimated as the size of the largest segment of a cyclotron circle that can be inscribed in the sample: $l_b^{(2)} \sim \sqrt{R_c W}$. Interparticle collisions lead only to small corrections to all observable quantities. Since the initial and the final angles of the electron velocity on such trajectories satisfy the condition $|\pi/2 - |\varphi|| \sim W/l_b^{(2)}$, the current is given by the formula similar to the one of the first ballistic subregime: $j = (2j_0/\pi) \ln(1/\sqrt{\omega_c W})$ [31]. The Hall field E_H becomes or the order of E_0 , like as in the near-edge regions in the first ballistic regime. The longitudinal and the Hall resistances acquire a non-trivial singular behavior as functions of B due to the factor $1/\ln(\sqrt{R_c/W})$ [see Fig. 3]. Similar behavior of the Hall resistance was previously obtained in numerical simulation of the ballistic transport and named the ballistic magnetoresistance anomaly [30].

In the third ballistic subregion, $\gamma W^2 \ll 2R_c - W \lesssim W$,

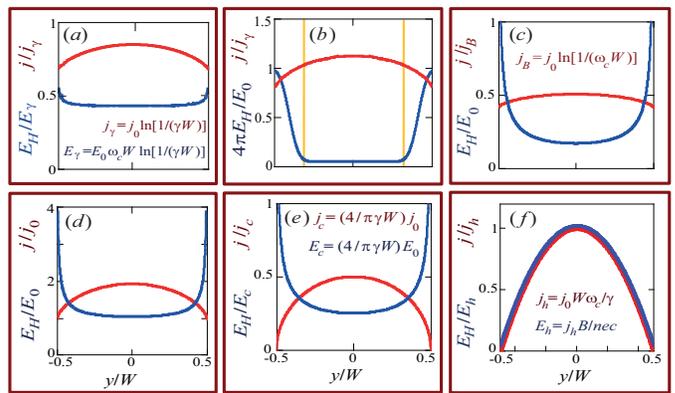


FIG. 2: Current density $j(y)$ and Hall electric field $E_H(y)$ at various magnetic fields B in: (a) the first ballistic subregime, the very limit $B \rightarrow 0$ (only the flow in the central part of the sample, $W/2 - |y| \gg \omega_c/\gamma^2$, is shown); (b) in the middle part of the first ballistic subregime, $R_c \gg l^2/W$ [schematically; vertical orange lines depict the boundaries of the near edge regions, $y_c \approx \pm(W/2 - \omega_c/\gamma^2)$]; (c) the second ballistic subregime, $W \ll R_c \ll l^2/W$; (d) the third ballistic subregime, $W < 2R_c$ provided $W \sim R_c$; (e) the very point of the ballistic-hydrodynamic phase transition, $W = 2R_c$; and (f) the hydrodynamic regime with a well-formed Poiseuille flow, $W \gg R_c$ (schematically).

only few electrons after a reflection from an edge reach the opposite edge [see Fig. 1(b)]. The most of electrons are moving by the skipping trajectories, those after the reflection from an edge are returning to the same edge. Herewith only the electrons of the first type, centers of whose orbits are located near the sample center $y = 0$, do compensate the kinematic contribution to the current j_y (the $\mathbf{E}_0 \times \mathbf{B}$ -drift). Since the reflection of electrons from the boundaries occurs with equal probability at all φ , the number of nonequilibrium electrons of both types increases greatly [31]. The main contributions to the current density j and the Hall field E_H are due to the skipping electrons, and the magnitudes of j and E_H rapidly increase with approaching of the difference $B_c - B$ to zero.

It is seen from Fig. 2(c,d) that in the second and the third ballistic subregimes the profiles $j(y)$ and $E_H(y)$ become more and more curved as compared with the first one. The singularities of $E_H(y)$ near the edges are due to a large number of electron in the vicinities of the edges moving almost along them relatively long times (see Fig. 1).

3. Phase transition. At high magnetic fields, $B > B_c$, corresponding to $W > 2R_c$, electrons are divided into two groups: the edge electrons that move predominantly along the skipping orbits intersecting one of the edges, and the central electrons whose trajectories do not touch the edges [see Figs. 1(c)]. The central electrons collide mainly with the edge electrons anticipating the formation of the bulk phase of the hydrodynamic electrons at $W \gg$

R_c . Our main goal is to show that in the vicinity of the critical field $B = B_c$ a phase transition occurs between almost independent ballistic electrons and a fluid phase of central electrons.

Just below the transition when $0 < 2R_c - W \lesssim \gamma W^2$, the imbalance in the numbers of the left-edge and the right-edge electrons on the skipping trajectories increases dramatically [31]. The densities of those electrons and their contributions to the current becomes to be controlled not only by their rare collisions with the opposite edges, but also by their collisions with other electrons. The values of j and E_H rapidly grows with approaching of W/R_c to two and become proportional to the scattering time $1/\gamma$ at $2 - W/R_c \sim \gamma W$ [see Fig. 2(e)].

Above the transition point, at $W > 2R_c$, the relative density $\alpha_c = n_c/n$ the central electrons depends on magnetic field as: $\alpha_c = (W - 2R_c)/W$ [see Fig. 1 (c)]. When $\alpha_c \ll 1$ and the proportion of the edge electrons is close to unity, $\alpha_e \equiv n_e/n = 1 - \alpha_c$, the central electrons lose their momenta predominantly via scattering on the edge electrons. Therefore the dynamics of the central electrons is similar to the particles in Ohmic flow in the reference frame moving with the mean velocity of the edge electrons. The distribution function of the first ones contains only several substantial harmonics by the velocity angle φ , unlike the ballistic distribution function at $B < B_c$ in which many harmonics are comparable. This indicates that the central electrons is a nucleus of the thermodynamic fluid phase, strongly different from the collective of ballistic electrons.

Such a change in the electron dynamics above and below the transition leads to a kink in the magnetic field dependencies of resistances $\varrho_{xx}(B)$ and $\varrho_{xy}(B)$ [31] (see Fig. 3). The kinks are the evidence that the formation of the hydrodynamic flow from the ballistic one is a phase transition. The relative density of the central electrons, α_c , can be considered as the order parameter of this transition. In the lower vicinity of the transition, $0 < B_c - B \ll B_c$, the ballistic electrons on skipping trajectories close to whole circles, having the momentum relaxation time $\sim 1/\gamma$, are a precursor of the transition.

With the increase of magnetic field, the relative density of the central electrons increases and their collisions with each other become important. At $\alpha_c \sim 1$, the current density of central electrons becomes y -dependent: the closer is a center of electron trajectories to the sample center, $y = 0$, the less important is its scattering on the edge electrons and more important is its scattering on other central electrons. When the cyclotron radius becomes very small, $R_c \ll W$, the central electrons dominate everywhere except the vicinities of the edges, $W/2 - |y| \sim R_c$ [see Fig. 2(d)]. In such well-formed Poiseuille flow, both functions $j(y)$ and $E_H(y)$ are parabolic, excepting for the narrow near-edge regions [see Fig. 2(d)]. The longitudinal resistance ϱ_{xx} is now determined by viscosity, $\varrho_{xx} \sim \eta_{xx}$, where $\eta_{xx} \sim \gamma/\omega_c^2$ is

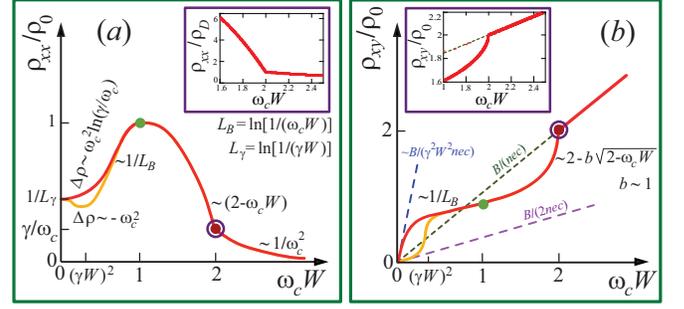


FIG. 3: Longitudinal ϱ_{xx} (a) and Hall ϱ_{xy} (b) resistances as functions of magnetic field normalized on the constant $\varrho_0 = mW/(ne^2)$. The asymptotic behaviors of the dependencies $\varrho_{xx}(\omega_c)$ and $\varrho_{xy}(\omega_c)$ in special regions are depicted near the transition point $\omega_c W = 2$. In the first ballistic region ($R_c \gg l^2/W$) the resistances of the whole sample including the near-edge regions (red curves) as well as of the bulk part of the sample (orange curves) are drawn.

the diagonal viscosity coefficient, whereas the Hall resistance ϱ_{xy} turns out to be close to the conventional Ohmic value $\varrho_{xy}^0 = R_H^0 B$ [19].

In Supplementary information [31], we compare our results with preceding theoretical [25, 26] and experimental [8, 9, 18] works. We provide the evidences that the ballistic-hydrodynamic phase transition was observed in Refs. [8, 9, 18] for 2D electron flows in high-quality graphene stripes and GaAs quantum well samples. In particular, the experimental dependencies $\varrho_{xx}(B)$ and $\varrho_{xy}(B)$ observed in Refs. [8, 9, 18] and in Ref. [18], respectively, very well correspond to the ones shown in Fig. 3. The specific shape of the longitudinal magnetoresistance $\varrho_{xx}(B)$ [see Fig. 3(a)] and experimental manifestations of a similar magnetoresistance in samples with hydrodynamic electrons allow to consider it as a characteristic sign of the ballistic-hydrodynamic phase transition.

4. Methods. Quantitatively, we describe the ballistic-hydrodynamic phase transition by a mean-field-like model which is based on the consideration of Refs. [28, 29]. The model takes into account the diffusive scattering of electrons on the sample edges and weak inter-particle collisions conserving momentum within a simplified kinetic equation [31]. In the ballistic regime, $B < B_c$, the departure part of the collision operator dominates. In the vicinity of the phase transition point, $B = B_c$, both the departure and the arrival terms of the collision operator becomes of the same order of magnitude. For such B , a mean-field-like simplification of the kinetic equation is proposed in which the arrival term is approximated by its averaged value over the sample cross section. Such kinetic equation preserves momentum and the number of particles in collisions only in the whole sample, but not at each point y .

The current density, calculated within our model in the

lower vicinity of the transition point, $2 - W/R_c \lesssim \gamma W$ in the main order by the difference $2R_c - W$ and the parameter γW has the form of a semicircle [see Fig. 2(c)]:

$$j(y) = j_c \sqrt{1 - (y/R_c)^2}. \quad (2)$$

Here $j_c = 4ne^2 E_0 / [\pi m(\gamma + 2\varepsilon)]$ is the current amplitude and $\varepsilon = (2 - W/R_c)v_F / (\pi R_c) \ll \omega_c$ is the parameter characterizing the proximity to the transition point. Current density (2) originates from the redistribution of electrons at the skipping orbits near the left and the right sample edges. We see from Eq. (2) that at $B \rightarrow B_c$ and $\varepsilon \rightarrow 0$ the current amplitude j_c diverges, and its maximum value is limited by the scattering rate. The corresponding Hall electric field in the main order by ε and γW takes the form:

$$E_H(y) = \frac{E_c}{\sqrt{1 - (y/R_c)^2}}, \quad (3)$$

where $E_c = 2E_0\omega_c / [\pi(\gamma + 2\varepsilon)]$.

Transformation of the dynamics of the edge electrons with crossing the critical magnetic field $B = B_c$ and the emergence of the central electrons at $B > B_c$ lead to a nonanalytical behavior of all macroscopic quantities (see Fig. 3). In particular, the averaged by y current density $j(B)$ and the Hall field $E_H(B)$ exhibit kinks at $B = B_c$. For the longitudinal $\varrho_{xx} = E_0/j$ and the Hall $\varrho_{xy} = E_H/j$ resistances in the vicinity of the ballistic-hydrodynamic phase transition, $|W/R_c - 2| \lesssim \gamma W$ we obtained [31]:

$$\varrho_{xx}(B) = \frac{m}{n_0 e^2} \begin{cases} \gamma + 2\varepsilon, & B < B_c \\ \gamma(1 - 2\alpha_c), & B > B_c \end{cases} \quad (4)$$

and

$$\varrho_{xy}(B) = \frac{B}{n_0 e c} \begin{cases} 1 - \sqrt{2\varepsilon/\pi}, & B < B_c \\ 1, & B > B_c \end{cases}. \quad (5)$$

It is noteworthy that the Hall constant $R_H(B) = \varrho_{xy}(B)/B$ right above the transition coincides with its value in the Ohmic regime at zero temperature, $R_H^0 = 1/(n_0 e c)$, at least, in the main order by γW in which all our calculations are performed.

5. Conclusion. A phase transition between the ballistic and the hydrodynamic regimes of transport is revealed and studied for 2D electrons in long samples in magnetic field. This effect can be considered as a simplest example of a sharp emergence of the phase of a charged viscous fluid. Possibly, similar scenarios of the ballistic-hydrodynamic transitions are realized in a wider class of high-mobility conductors.

We thank A. I. Chugunov, L. E. Golub, and A. V. Shumilin for fruitful discussions. The study was supported by the Russian Fund for Basic Research (Grant No. 19-02-00999) and by the Foundation for the Advancement of Theoretical Physics and Mathematics "BASIS".

-
- [1] R. N. Gurzhi, Hydrodynamic effects in solids at low temperatures, *Sov. Phys. Uspekhi* **94**, 657 (1968).
 - [2] M. Hruska and B. Spivak, Conductivity of the classical two-dimensional electron gas, *Phys. Rev. B* **65**, 033315 (2002).
 - [3] P. J. W. Moll, P. Kushwaha, N. Nandi, B. Schmidt, and A. P. Mackenzie, Evidence for hydrodynamic electron flow in PdCoO₂, *Science* **351**, 1061 (2016).
 - [4] D. A. Bandurin, I. Torre, R. Krishna Kumar, M. Ben Shalom, A. Tomadin, A. Principi, G. H. Auton, E. Khestanova, K. S. Novoselov, I. V. Grigorieva, L. A. Ponomarenko, A. K. Geim, and M. Polini, Negative local resistance caused by viscous electron backflow in graphene, *Science* **351**, 1055 (2016).
 - [5] L. Levitov and G. Falkovich, Electron viscosity, current vortices and negative nonlocal resistance in graphene, *Nature Physics* **12**, 672 (2016).
 - [6] R. Krishna Kumar, D. A. Bandurin, F. M. D. Pellegrino, Y. Cao, A. Principi, H. Guo, G. H. Auton, M. Ben Shalom, L. A. Ponomarenko, G. Falkovich, K. Watanabe, T. Taniguchi, I. V. Grigorieva, L. S. Levitov, M. Polini, and A. K. Geim, Superballistic flow of viscous electron fluid through graphene constrictions, *Nature Physics* **13**, 1182 (2017).
 - [7] A. I. Berdyugin, S. G. Xu, F. M. D. Pellegrino, R. Krishna Kumar, A. Principi, I. Torre, M. Ben Shalom, T. Taniguchi, K. Watanabe, I. V. Grigorieva, M. Polini, A. K. Geim, and D. A. Bandurin, Measuring Hall viscosity of graphene's electron fluid, *Science* **364**, 162 (2019).
 - [8] J. A. Sulpizio, L. Ella, A. Rozen, J. Birkbeck, D. J. Perello, D. Dutta, M. Ben-Shalom, T. Taniguchi, K. Watanabe, T. Holder, R. Queiroz, A. Principi, A. Stern, T. Scaffidi, A. K. Geim, and S. Ilani, Visualizing Poiseuille flow of hydrodynamic electrons, *Nature* **576**, 75 (2019).
 - [9] M. J. H. Ku, T. X. Zhou, Q. Li, Y. J. Shin, J. K. Shi, C. Burch, L. E. Anderson, A. T. Pierce, Y. Xie, A. Hamo, U. Vool, H. Zhang, Francesco Casola, T. Taniguchi, K. Watanabe, M. M. Fogler, P. Kim, A. Yacoby, and R. L. Walsworth, Imaging viscous flow of the Dirac fluid in graphene, *Nature* **583**, 537 (2020).
 - [10] J. Gooth, F. Menges, C. Shekhar, V. Suess, N. Kumar, Y. Sun, U. Drechsler, R. Zierold, C. Felser, and B. Gotsmann, Thermal and electrical signatures of a hydrodynamic electron fluid in tungsten diphosphide, *Nature Communications* **9**, 4093 (2018).
 - [11] L. Bockhorn, P. Barthold, D. Schuh, W. Wegscheider, and R. J. Haug, Magnetoresistance in a high-mobility two-dimensional electron gas, *Phys. Rev. B* **83**, 113301 (2011).
 - [12] A. T. Hatke, M. A. Zudov, J. L. Reno, L. N. Pfeiffer, and K. W. West, Giant negative magnetoresistance in high-mobility two-dimensional electron systems, *Phys. Rev. B* **85**, 081304 (2012).
 - [13] R. G. Mani, A. Kriisa, and W. Wegscheider, Size-dependent giant-magnetoresistance in millimeter scale GaAs/AlGaAs 2D electron devices, *Scientific Reports* **3**, 2747 (2013).
 - [14] Q. Shi, P. D. Martin, Q. A. Ebner, M. A. Zudov, L. N. Pfeiffer, and K. W. West, Colossal negative magnetoresistance in a two-dimensional electron gas, *Phys. Rev. B*

- 89**, 201301 (2014).
- [15] L. Bockhorn, I. V. Gornyi, D. Schuh, C. Reichl, W. Wegscheider, and R. J. Haug, Magnetoresistance induced by rare strong scatterers in a high-mobility two-dimensional electron gas *Phys. Rev. B* **90**, 165434 (2014).
 - [16] G. M. Gusev, A. D. Levin, E. V. Levinson, and A. K. Bakarov, Viscous electron flow in mesoscopic two-dimensional electron gas, *AIP Advances* **8**, 025318 (2018).
 - [17] A. D. Levin, G. M. Gusev, E. V. Levinson, Z. D. Kvon, and A. K. Bakarov, Vorticity-induced negative nonlocal resistance in a viscous two-dimensional electron system, *Phys. Rev. B* **97**, 245308 (2018).
 - [18] G. M. Gusev, A. D. Levin, E. V. Levinson, and A. K. Bakarov, Viscous transport and Hall viscosity in a two-dimensional electron system, *Phys. Rev. B* **98**, 161303 (2018).
 - [19] P. S. Alekseev, Negative Magnetoresistance in Viscous Flow of Two-Dimensional Electrons, *Phys. Rev. Lett.* **117**, 166601 (2016).
 - [20] Y. Dai, R. R. Du, L. N. Pfeiffer, and K. W. West, Observation of a Cyclotron Harmonic Spike in Microwave-Induced Resistances in Ultraclean GaAs/AlGaAs Quantum Wells, *Phys. Rev. Lett.* **105**, 246802 (2010).
 - [21] A. T. Hatke, M. A. Zudov, L. N. Pfeiffer, and K. W. West, Giant microwave photoresistivity in high-mobility quantum Hall systems, *Phys. Rev. B* **83**, 121301 (2011).
 - [22] M. Bialek, J. Lusakowski, M. Czapkiewicz, J. Wrobel, and V. Umansky, Photoresponse of a two-dimensional electron gas at the second harmonic of the cyclotron resonance, *Phys. Rev. B* **91**, 045437 (2015).
 - [23] P. S. Alekseev and A. P. Alekseeva, Transverse Magnetosonic Waves and Viscoelastic Resonance in a Two-Dimensional Highly Viscous Electron Fluid, *Phys. Rev. Lett.* **123**, 236801 (2019).
 - [24] H. Guo, E. Ilseven, G. Falkovich, and L. Levitov, Higher-than-ballistic conduction of viscous electron flows, *PNAS* **114**, 3068 (2017).
 - [25] T. Scaffidi, N. Nandi, B. Schmidt, A. P. Mackenzie, and J. E. Moore, Hydrodynamic Electron Flow and Hall Viscosity, *Phys. Rev. Lett.* **118**, 226601 (2017).
 - [26] T. Holder, R. Queiroz, T. Scaffidi, N. Silberstein, A. Rozen, J. A. Sulpizio, L. Ella, S. Ilani, and A. Stern, Ballistic and hydrodynamic magnetotransport in narrow channels, *Phys. Rev. B* **100**, 245305 (2019).
 - [27] E. M. Baskin, L. N. Magarill, and M. V. Entin, Two-dimensional electron-impurity system in a strong magnetic field, *Sov. Phys. JETP* **48**, 365 (1978).
 - [28] P. S. Alekseev and M. A. Semina, Ballistic flow of two-dimensional interacting electrons, *Phys. Rev. B* **98**, 165412 (2018).
 - [29] P. S. Alekseev and M. A. Semina, Hall effect in a ballistic flow of two-dimensional interacting particles, *Phys. Rev. B* **100**, 125419 (2019).
 - [30] C. W. J. Beenakker and H. van Houten, Quantum Transport in Semiconductor Nanostructures, *Solid State Physics* **44**, 1 (1991).
 - [31] For the details of the model and of the calculations as well as for the detailed comparison with preceding works see Supplementary information below.

Supplementary information to “Theory of ballistic-hydrodynamic phase transition in flow of two-dimensional electrons”

A. N. Afanasiev, P. S. Alekseev, A. A. Greshnov, and M. A. Semina

Ioffe Institute, Politekhnikeskaya 26, 194021, St. Petersburg, Russia

Here we present the details of our theoretical model, the mathematical method of the solution of its equations, and of derivation of the properties of the electron flow below and above the ballistic-hydrodynamic phase transition. We also compare our results with the results of preceding theoretical and experimental studies.

1. MODEL

In order to study the transitions from the ballistic regime of 2D electron transport to the hydrodynamic or the Ohmic ones, we consider a flat flow in a long sample with the width W and the length $L \gg W$ with the rough longitudinal edges (see Fig. 1 in the main text). Here-with we use the simplified forms of the electron-electron and the disorder collision integrals, allowing the analytical solution of the kinetic equation. Such model has been developed in Refs. [28, 29] to study the ballistic transport of 2D interacting electrons in the limit of very low magnetic field, $B \rightarrow 0$ (here and below citations [1], [2], and so on refer to the bibliography of the main text).

We seek for the linear response to a homogeneous electric field $\mathbf{E}_0 \parallel x$ in the presence of external magnetic field \mathbf{B} perpendicular to the sample plane (see Fig. 1 in the main text). The corresponding distribution function of 2D electrons acquires a nonequilibrium part:

$$\delta f(y, \mathbf{p}) = -f'_F(\varepsilon) f(y, \varphi, \varepsilon) \sim E_0, \quad (\text{S1})$$

where $f_F(\varepsilon)$ is the Fermi distribution function, $\varepsilon = p^2/(2m)$ is the electron energy, φ is the angle of the electron velocity $\mathbf{v} = v(\varepsilon)[\sin \varphi, \cos \varphi]$ and the normal to the left sample edge (see Fig. 1 in the main text), $\mathbf{p} = m\mathbf{v}$ is the electron momentum, and m is the electron mass. The dependence of δf on the coordinate x is absent since $L \gg W$. We also omit the energy dependence of the electron velocity $v(\varepsilon) = \sqrt{2\varepsilon/m}$ and of the factor $f(y, \varphi, \varepsilon)$ in the nonequilibrium part of distribution function $\delta f(y, \mathbf{p})$. This simplification is apparently valid for the 2D electrons degenerate electrons interacting by Coulomb's law when the charge transport is studied. Hereinafter, we use the units of all values in which the characteristic electron velocity $v(\varepsilon) \equiv v_F$ and the electron charge e are set to be unity. Therefore, coordinate, time, and reciprocal electric field, $1/E_0$, have the same units.

The kinetic equation for the inequilibrium distribution function $f(y, \varphi)$ takes the form:

$$\cos \varphi \frac{\partial f}{\partial y} - \sin \varphi E_0 - \cos \varphi E_H - \omega_c \frac{\partial f}{\partial \varphi} = \text{St}[f], \quad (\text{S2})$$

where $\omega_c = eB/mc$ is the cyclotron frequency, E_H is the Hall electric field arising due to redistribution of particles in the presence of magnetic field, and the collision integral $\text{St}[f]$ describes both momentum-conserving electron-electron collisions and dissipative scattering by the bulk disorder. We use the following simplified form of $\text{St}[f]$:

$$\text{St}[f] = -\gamma f + \gamma_{ee} \hat{P}[f] + \gamma_d \hat{P}_0[f], \quad (\text{S3})$$

where γ_{ee} and γ_d are electron-electron and disorder scattering rates, $\gamma = \gamma_{ee} + \gamma_d$ is the total scattering rate, \hat{P} and \hat{P}_0 are the projector operators of the functions $f(\varphi)$ onto the subspaces $\{1, e^{\pm i\varphi}\}$ and $\{1\}$, respectively. Such collision integral conserves perturbations of the distribution function corresponding to a nonequilibrium density. It also describes the conservation of momentum in the processes of inter-particle collisions.

We consider that the longitudinal sample edges are rough. Thus the scattering of electrons on the edges is diffusive and the boundary conditions for the distribution function takes the form [30],[29]:

$$\begin{aligned} f(-W/2, \varphi) &= c_l, \quad -\pi/2 < \varphi < \pi/2, \\ f(W/2, \varphi) &= c_r, \quad \pi/2 < \varphi < 3\pi/2, \end{aligned} \quad (\text{S4})$$

see Fig. 1 in the main text. Here the quantities $c_l = c_l[f]$ and $c_r = c_r[f]$ are proportional to the y components of the incident particle flow on the left ($y = -W/2$) and the right ($y = W/2$) sample edges:

$$\begin{aligned} c_l &= -\frac{1}{2} \int_{\pi/2}^{3\pi/2} d\varphi' \cos \varphi' f(-W/2, \varphi'), \\ c_r &= \frac{1}{2} \int_{-\pi/2}^{\pi/2} d\varphi' \cos \varphi' f(W/2, \varphi'). \end{aligned} \quad (\text{S5})$$

These boundary conditions indicate that (i) the probability of electron reflection from the rough sample edge is independent on the reflection angle φ and (ii) the transverse component of the electron flow,

$$j_y(y) = \frac{n_0}{\pi m} \int_0^{2\pi} d\varphi' \cos \varphi' f(y, \varphi'), \quad (\text{S6})$$

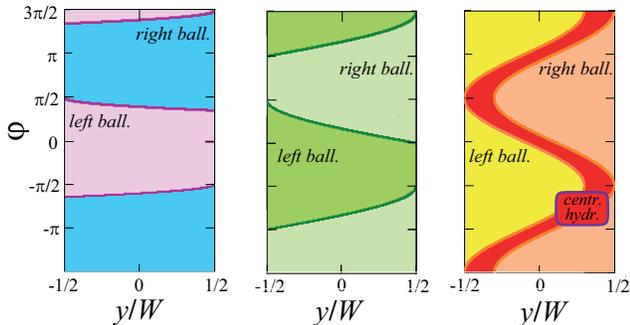


FIG. S1: Regions in the plane (y, φ) corresponding to the trajectories of the ballistic electrons, reflected from the left and the right sample edges (in all panels), as well as of the central hydrodynamic electrons, those do not scatter on the edges [red region in panel (c)]. The cases of narrow, $W \ll R_c$ (a); intermediate, $W \sim R_c$ (b); and wide, $W > 2R_c$ (c) are shown.

vanishes at the edges, $j_y|_{y=\pm W/2} = 0$, and, thus, everywhere in the sample due to the continuity equation $\text{div } \mathbf{j} = j' = 0$.

The longitudinal current density along the sample is defined as:

$$j(y) \equiv j_x(y) = \frac{n_0}{\pi m} \int_0^{2\pi} d\varphi' \sin \varphi' f(y, \varphi'). \quad (\text{S7})$$

If an electric current flows through a sample in a magnetic field, a perturbation of the charged density and the Hall electric field arise due to the magnetic Lorentz force. Both these effects are described by the zeroth ($m = 0$) angular harmonic of the distribution function:

$$f^{m=0}(y) = \frac{1}{2\pi} \int_0^{2\pi} d\varphi' f(y, \varphi'). \quad (\text{S8})$$

Figures S1(a,b) shows the regions in the (y, φ) -plane corresponding to the ballistic motion of electrons reflected from the right and from the left sample edges. Here and below in the current work we imply that the electron mean free path $l = 1/\gamma$ is much longer than the sample width. Therefore, most of electrons are not scattering in the bulk and move inside the left or inside the right regions between collisions with the edges.

For narrow samples, $W \ll R_c$, the left and the right ballistic regions are close to the rectangles $[-\pi/2, \pi/2] \times [-W/2, W/2]$ and $[\pi/2, 3\pi/2] \times [-W/2, W/2]$ [see Fig. S1(a)]. For wider samples, $W \sim R_c$, $W < 2R_c$, the boundaries of the left and right region $\varphi_{\pm}(y)$ begin to significantly depend on coordinate y [see Fig. S1(b)]. The very boundary curves $\varphi_{\pm}(y)$ coincide the electron trajectories those are touching the edges tangentially. Therefore the distribution function $f(y, \varphi)$ is not well defined at $\varphi = \varphi_{\pm}(y)$ and can have a discontinuity at these curves. At magnetic fields above the

critical field, $W > 2R_c$, the central electrons those do not scatter on the edges arise in the region filled with red in Fig. S1(c). Herewith the edge electrons in the left and right regions (yellow and pink) still scatter mainly on the edges.

It is useful to rewrite the kinetic equation (S2) in the form:

$$\begin{aligned} & \left[\cos \varphi \frac{\partial}{\partial y} + \gamma \right] \tilde{f} - \sin \varphi E_0 = \\ & = \gamma_{ee} \hat{P}[\tilde{f}] + \gamma_d \hat{P}_0[\tilde{f}] + \omega_c \frac{\partial \tilde{f}}{\partial \varphi}, \end{aligned} \quad (\text{S9})$$

where we have introduced the function:

$$\tilde{f}(y, \varphi) = f(y, \varphi) + \phi(y). \quad (\text{S10})$$

Here, ϕ is the electrostatic potential of the Hall electric field $E_H = -\phi'$. Indeed, it follows from Eq. (S2) that the Hall potential $\phi(y)$ plays the same role in the transport equation as its progenitor, the zero harmonic of the distribution function $f^{m=0}(y)$ (S8) being proportional to the inhomogeneous density perturbations. Therefore it is reasonable to introduce the function $\tilde{f}(y, \varphi)$ (S10) in order to take into account $\phi(y)$ and $f^{m=0}(y)$ within the same framework.

The zero harmonic $\tilde{f}^{m=0}(y)$ of the generalized distribution function (S10) takes the form:

$$\tilde{f}^{m=0}(y) = \delta\mu(y) + \phi(y), \quad (\text{S11})$$

where $\delta\mu$ is the perturbation of the electron chemical potential. In the case of sufficiently slow flows, the values $\delta\mu(y)$ and $\phi(y)$ are related by the electrostatic relations [23]. For the considered case of 2D identical degenerate electrons, the electrostatic potential ϕ is usually much greater than the corresponding perturbation of the chemical potential $\delta\mu$ [23]. Thus the Hall electric field is calculated just by the formula $E_H(y) \approx -[\tilde{f}^{m=0}]'(y)$.

For brevity, we further omit the tilde in the function \tilde{f} and write $f \equiv \tilde{f}$.

2. SOLUTION OF KINETIC EQUATION IN BALLISTIC REGIME

2.1. General solution

In this section we consider the 2D electron transport in a long sample in relatively weak magnetic fields when the diameter of the cyclotron circle larger than the sample width, $2R_c > W$. Provided the mean free path is much longer than the sample width, $l = 1/\gamma \gg W$, the dominant mechanism of scattering of the most of electrons is collisions with the sample edges.

In Ref. [28] the kinetic equation (S9) in the limits $\gamma W \gg 1$ and $\gamma W \ll 1$ at zero magnetic field was analyzed. First, it was demonstrated that the hydrodynamic regime is realized in the limit $\gamma W \gg 1$ in the central region of the sample, $W/2 - |y| \gg 1/\gamma$. In this domain, both sides of Eq. (S9) are of the same order of magnitude and it is transformed into the Navier-Stokes equation for the density of the electron flow $j_x(y)$.

Second, it was shown in Ref. [28] that in the ballistic regime, $\gamma W \ll 1$, the terms $\cos \varphi \partial f / \partial y$ and $\sin \varphi E_0$ in the left-hand side of Eq. (S9) are much larger than the arrival terms $\gamma_{ee} \hat{P}[f]$ and $\gamma_d \hat{P}_0[f]$ in the right-hand side in the factor of $\ln[1/(\gamma W)]$, therefore the last terms can be taking into account in the solution by the perturbation theory. Herewith the departure term γf in the left-hand side plays role of regularization of the kinetic equation near the angles $\varphi \approx \pm \pi/2$, where the cosine factor in the term $\cos \varphi \partial f / \partial y$ is close to zero.

In Ref. [29] the similar result for equation (S9) at a nonzero magnetic field was obtained. Namely, in weak magnetic fields, $\omega_c \ll \gamma^2 W$, the terms $\gamma_{ee} \hat{P}[f]$ and $\gamma_d \hat{P}_0[f]$ should be treated as perturbations in the equations for the first, $f_1 \sim \omega_c$, and the second, $f_2 \sim \omega_c^2$, order corrections by magnetic field to the distribution function $f(y, \varphi)$, those are responsible for the Hall effect and the magnetoresistance in the ballistic regimes.

Next, it is reasonable to expect that in narrow samples, $\gamma W \ll 1$, at intermediate magnetic field,

$$\omega_c \sim 1/W, \quad \omega_c < 2/W, \quad (\text{S12})$$

the vanishing of the term $\cos \varphi \partial f / \partial y$ at $|\varphi| \approx \pi/2$ is ‘‘healed’’ by the magnetic field term $\omega_c \partial f / \partial \varphi$ and the electron flow is mainly determined by the electron collisions with the edges. The neglect of the collision terms in kinetic equation (S9) leads to the following estimates:

$$f \sim \frac{E_0}{\omega_c}, \quad j \sim j_0, \quad E_H \sim E_0. \quad (\text{S13})$$

In these formulas we have introduced the typical amplitude of the current density, $j_0 = n_0 E_0 W / m$. According to such estimate of f , both the arrival and the departure terms are proportional to $(\gamma / \omega_c) E_0 \ll E_0$ and thus are much smaller than the other terms of Eq. (S9). Consequently, in this regime the bulk collision terms in kinetic equation (S9) seem to lead only to small corrections to the distribution function, being proportional to the small parameter γ / ω_c .

Below we will see that above estimations (S13) are indeed valid at $\omega_c < 2/W$ except the region of very weak magnetic fields and the region near the phase transition. The first one, $\omega_c \ll 1/W$, was partly studied in Refs. [28],[29]. In it, the maximum length of the ballistic trajectories is achieved for electrons moving almost along the sample. In the second one, $0 < 2 - \omega_c W \lesssim \gamma W$, the electron-electron collisions and/or scattering on the bulk

disorder provide the contribution to relaxation processes comparable with the scattering on the edges, thus this is already not the ballistic regime.

In this way, the ballistic regime, being realized in the interval $\gamma W \ll 2 - \omega_c W < 2$ (we assume that $\omega_c > 0$), is divided on the three subregimes:

$$(i) \quad \omega_c \ll \gamma^2 W \quad (\text{S14})$$

{the case partly studied in Refs. [28, 29], in which the length $l_b^{(2)} = \sqrt{R_c W}$ of the maximal segment of a cyclotron circle that can be inscribed in the stripe is longer than the mean free path relative to the bulk scattering, $l_b^{(2)} \gg l = 1/\gamma$, therefore the longest ballistic trajectories are confined by the bulk scattering};

$$(ii) \quad \gamma^2 W \ll \omega_c \ll 1/W \quad (\text{S15})$$

[the magnetic field parameter $\omega_c W$ is small; the maximal trajectory length is limited by cyclotron rotation: $l_b^{(2)} \ll 1/\gamma$; and the bulk scattering provides only small corrections (the last fact is consistent with the above estimations and will be proved in another publication, see also Section 2.2 below)]; and

$$(iii) \quad \omega_c \sim 1/W, \quad 2 - \omega_c W \gg \gamma W \quad (\text{S16})$$

[the case when $l_b^{(2)} \ll 1/\gamma$, the magnetic field parameter $\omega_c W$ is of order of unity or is close to its critical value, $\omega_c W = 2$; and the bulk scattering still provides only small corrections to all values].

According to the results of Refs. [28, 29] for the case (i) and the above estimations characterizing the cases (ii) and (iii), in order to develop a unified description of the ballistic transport in all the subregimes (i)-(iii) one should use kinetic equation (S9) retaining only the departure collision term:

$$\left[\cos \varphi \frac{\partial}{\partial y} + \gamma \right] f - \sin \varphi e E_0 = \omega_c \frac{\partial f}{\partial \varphi}. \quad (\text{S17})$$

This equation can be solved by the method of characteristics.

Such solution was constructed in recent publication [26]. In our work, using a slightly different approach, we obtain the ballistic distribution function $f(y, \varphi)$ similar to the one obtained in Ref. [26]. We use this solution to study the regimes those were not considered in Ref. [26]: the first ballistic subregime, $\omega_c W \ll \gamma^2 W^2$, (partly studied in Refs. [28],[29]) and the singular part of the third subregime (iii), $\gamma W \ll 2 - \omega_c W \ll 1$.

The solution of Eq. (S17) with boundary conditions (S4) and (S5) is a discontinuous function with the domains of continuity shown in Figs. S1(a,b). For the electrons reflected from the left edge, whose trajectories lie in the diapason:

$$-\pi + \arcsin[1 - \omega_c (W/2 - y)] < \varphi < \arcsin[1 - \omega_c (W/2 + y)], \quad (\text{S18})$$

[see Fig. S1(a,b)] we introduce the following notation for the electron distribution function: $f(y, \varphi) = f_+(y, \varphi)$. For the electrons reflected from the right edge, whose trajectories are located in the diapason

$$\begin{aligned} \arcsin[1 - \omega_c(W/2 + y)] < \varphi < \\ < \pi + \arcsin[1 - \omega_c(W/2 - y)], \end{aligned} \quad (\text{S19})$$

[see Fig. S1(a,b)] we use the analogous notation: $f(y, \varphi) = f_-(y, \varphi)$. The functions f_{\pm} are found by the standard method of characteristic for the first-order differential equation (S17). After standard, but lengthy calculations we obtain:

$$\begin{aligned} f_{\pm}(y, \varphi) = \frac{E_0}{\gamma^2 + \omega_c^2} \left[\omega_c \cos \varphi + \gamma \sin \varphi + \right. \\ \left. + e^{\gamma \varphi / \omega_c} Z_{\pm}(\sin \varphi + \omega_c y) \right], \end{aligned} \quad (\text{S20})$$

where the y -independent terms $\omega_c \cos \varphi$ and $\gamma \sin \varphi$ are particular solutions of Eq. (S17) those corresponds to the usual Drude formulas (provided γ is rate of the bulk electron scattering), while the term $e^{\gamma \varphi / \omega_c} Z_{\pm}(X)$ is a general solution of kinetic equation (S17) [without the field term $\sin \varphi E_0$], allowing to satisfy the proper boundary conditions (S4).

By substituting Eq. (S20) into boundary conditions (S4), we obtain the explicit form of $Z_{\pm}(X)$:

$$\begin{aligned} Z_+(X) = e^{-\frac{\gamma}{\omega_c} \arcsin(X + \omega_c W/2)} \left[c_l - \right. \\ \left. - \gamma (X + \omega_c W/2) - \omega_c \sqrt{1 - (X + \omega_c W/2)^2} \right] \end{aligned} \quad (\text{S21})$$

and

$$\begin{aligned} Z_-(X) = e^{-\frac{\gamma}{\omega_c} [\pi - \arcsin(X - \omega_c W/2)]} \left[c_r - \right. \\ \left. - \gamma (X - \omega_c W/2) + \omega_c \sqrt{1 - (X - \omega_c W/2)^2} \right], \end{aligned} \quad (\text{S22})$$

where the coefficients c_l and c_r are determined from balance relations (S5) of the boundary conditions. The resulting linear equations for c_l and c_r takes the form:

$$\begin{pmatrix} I_{ll} & I_{lr} \\ I_{rl} & I_{rr} \end{pmatrix} \begin{pmatrix} c_l \\ c_r \end{pmatrix} = - \begin{pmatrix} I_l \\ I_r \end{pmatrix}, \quad (\text{S23})$$

where the coefficients in the first line of the matrix are expressed via the integrals:

$$I_{ll} = 2 + \int_{-\pi + \varphi_0}^{-\pi/2} d\varphi \cos \varphi e^{\frac{\gamma}{\omega_c} (\pi + 2\varphi)} \quad (\text{S24})$$

and

$$I_{lr} = \int_{\pi/2}^{\pi + \varphi_0} d\varphi \cos \varphi e^{\frac{\gamma}{\omega_c} [\varphi - \pi + \arcsin(\sin \varphi - \omega_c W)]}, \quad (\text{S25})$$

while the first components of the right-hand vector is:

$$\begin{aligned} I_l = \frac{\pi \omega_c}{2} + \int_{\varphi_0}^{\pi/2} d\varphi \cos \varphi \times \\ \times e^{\frac{\gamma}{\omega_c} (2\varphi - \pi)} (\omega_c \cos \varphi - \gamma \sin \varphi) - \\ - \int_{-\pi/2}^{\varphi_0} d\varphi \cos \varphi e^{\frac{\gamma}{\omega_c} [\varphi - \arcsin(\sin \varphi + \omega_c W)]} \times \\ [\omega_c \sqrt{1 - (\sin \varphi + \omega_c W)^2} + \gamma (\sin \varphi + \omega_c W)]. \end{aligned} \quad (\text{S26})$$

The other coefficients in Eq. (S23), I_{rr} , I_{rl} and I_r , are related to I_{ll} , I_{lr} , and I_l by the formulas:

$$I_{rr} = -I_{ll}, \quad I_{rl} = -I_{lr}, \quad I_r = I_l. \quad (\text{S27})$$

In Eqs. (S24)-(S26) we introduced the notation: $\varphi_0 = \arcsin(1 - \omega_c W)$.

At general values of the parameter $\omega_c W$, integrals (S24)-(S27) can be calculated only numerically. However, the explicit expressions for these integrals and the values $c_{l,r}$, $j(y)$, and $E_H(y)$ can be obtained in the limiting cases: $\omega_c W \ll (\gamma W)^2$ [the first ballistic subregion (i)]; $(\gamma W)^2 \ll \omega_c W \ll 1$ [the second ballistic subregion (ii)]; and $\gamma W < 2 - \omega_c W \ll 1$ [the right singular part of the third ballistic subregion (iii)].

2.2. Ballistic transport in moderate magnetic fields

Our preliminary estimates show that in the interval of magnetic fields $(\gamma W)^2 \ll \omega_c W \lesssim 1$ provided that $2 - \omega_c W \gg \gamma W$ [the second and the third ballistic sub-regimes] the electron flow in the main order by γ is determined by taking into account only the action of the external fields and the scattering on the rough edges.

Therefore, the asymptote of Eq. (S20) by $\gamma \rightarrow 0$ provides the proper distribution function in the main order by the parameter γW . Such distribution function takes the form:

$$\begin{aligned} f_{\pm}(y, \varphi) = \tilde{c}_{l,r} + \frac{E_0}{\omega_c} \left\{ \cos \varphi \mp \right. \\ \left. \mp \sqrt{1 - \left[\sin \varphi + \omega_c \left(y \pm \frac{W}{2} \right) \right]^2} \right\}, \end{aligned} \quad (\text{S28})$$

where $\tilde{c}_{l,r} = E_0 c_{l,r} / \omega_c^2$. The solution of Eq. (S20) at $\gamma = 0$ can be determined up to a constant term, that corresponds to the fact that function (S20) implies a weak artefact relaxation of the electron density due to the neglect of the term $\gamma P_0[f]$. Imposing the symmetric condition $c_l + c_r = 0$ corresponding to zero mean electron density in the sample, we obtain from system (S23):

$$\tilde{c}_{l,r} = \mp \frac{E_0}{\omega_c} \frac{U - V}{2(2 - \omega_c W)}, \quad (\text{S29})$$

where

$$\begin{aligned} U &= \arccos(1 - \omega_c W), \\ V &= (1 - \omega_c W) \sqrt{\omega_c W} \sqrt{2 - \omega_c W}. \end{aligned} \quad (\text{S30})$$

We note that solution (S28) has been obtained in recent work [26].

A detailed description of the profiles of the current $j(y)$ and the Hall field $E_H(y)$, the behavior of the longitudinal and the Hall resistances, as well as a detailed justification of the applicability of Eq. (S28) at the discussed moderately weak magnetic fields, $(\gamma W)^2 \ll \omega_c W \lesssim 1$, is planned to be published in another publication in the nearest future.

In this work we present only the simplest properties of the flow corresponding to the fully ballistic distribution function (S28). First of all, we note that solution (S28) implies that interparticle collisions provide only small corrections to all observable quantities. The main part of the current density $j(y)$ in the whole interval $(\gamma W)^2 \ll \omega_c W \lesssim 1$ is estimated as:

$$j \sim j_0 \ln \left(\frac{1}{\sqrt{\omega_c W}} \right), \quad (\text{S31})$$

where $\sqrt{\omega_c W} = W/l_b^{(2)}$ is the maximum possible angle between the sample direction x and the ballistic trajectories which intersect both sample edges (we remind that $l_b^{(2)} = \sqrt{WR_c}$). As it was discussed above and in the main text, Eq. (S31) expresses the fact that the ballistic trajectories providing the most important contribution to j are directed almost along the external electric field and have the lengths of the order of $l_b^{(2)}$. At the intermediate magnetic fields, $\omega_c \sim 1/W$, distribution function (S28) leads to the presented above estimate:

$$E_H \sim E_0 \quad (\text{S32})$$

for the Hall field [see Eq. (S13)].

In the vicinity the transition point, but not too close to it, $\gamma W \ll 2 - \omega_c W \ll 1$ [the right part of the third ballistic subregime], the coefficients $\tilde{c}_{l,r}$ diverge rapidly:

$$\tilde{c}_{l,r} = \pm \frac{\pi E_0}{2\omega_c(2 - \omega_c W)}. \quad (\text{S33})$$

They become greater than the other terms in Eq. (S28) and, thus, represent the main part of the distribution function. Such distribution function implies that there arises an imbalance between the densities of inquilinism electrons reflected from the left and from the right edges in order to compensate the part of the nonequilibrium flows j_y induced by the $E \times B$ -drift. Correspondingly, the magnitudes of j and E_H also diverge as $\sim 1/(2 - \omega_c W)$ at this near-transition fields $\gamma W \ll 2 - \omega_c W \ll 1$.

2.3. Ballistic transport in very weak magnetic fields

In the first ballistic subregime (i), $\omega_c \ll \gamma^2 W$, the continuity domains of $f_{\pm}(y, \varphi)$ given by Eqs. (S18) and (S19) become very close to $-\pi/2 < \varphi < \pi/2$ and $\pi/2 < \varphi < 3\pi/2$ at any y [see Fig. S1(a)]. The trajectories of the most of electrons are slightly bent lines starting on one edge and ending on another one.

In Refs. [28, 29] a solution of Eq. (S17) in the limit $\omega_c \rightarrow 0$ based on the perturbation theory by the magnetic field term was constructed. Up to the second order in ω_c , such distribution function has the form:

$$f = f_0 + f_1 + f_2, \quad (\text{S34})$$

where f_0 is the distribution function in zero magnetic field, while $f_1 \sim \omega_c$ and $f_2 \sim \omega_c^2$.

In this subsection, first, we refine the applicability of this approach of Refs. [28, 29]. Comparison of the magnetic field term, $\omega_c \partial f / \partial \varphi$, in the kinetic equation with any other term, for example, $\cos \varphi \partial f / \partial y$ at the angles $|\varphi| \rightarrow \pi/2$ shows that the effect from a magnetic field can be treated as a perturbation for electrons in the central bulk part of the sample:

$$W/2 - |y| \gg \omega_c / \gamma^2. \quad (\text{S35})$$

This leads to the power decomposition (S34) for the distribution function of such electrons and to the corresponding formulas for the contribution of region (S35) to j , E_H , and the averaged resistances (see Refs. [28, 29]). However, in the very vicinities of the sample edges,

$$W/2 - |y| \lesssim \omega_c / \gamma^2, \quad (\text{S36})$$

the magnetic field term $\omega_c \partial f / \partial \varphi$ cannot be treated as a perturbation for the electrons with $|\varphi| \approx \pi/2$ and the flow at such y and φ remains almost collisionless, being similar to the one studied in the previous subsection.

The criteria (S35) and (S36) can be also understood from the comparison of the two possible limitations for the lengths of the ballistic trajectories at $|\varphi| \rightarrow \pi/2$: the size $\sqrt{R_c(W/2 - |y|)}$ of the cyclotron circle segment having the height $(W/2 - |y|)$ and the bulk scattering length, $l = 1/\gamma$. In Refs. [28, 29] the possibility of forming of such near-edge regions where the perturbation theory by ω_c becomes not applicable was missed.

In realistic samples, the near-edges regions can be formed only in not too small magnetic field in the sample having very long and straight, but rough edges, namely when the critical width $(W/2 - |y|)_{crit} = \omega_c / \gamma^2$ is larger than the size of edges roughnesses. In any way, At very low fields inside the first subregime, $\omega_c < \omega_c^* \ll \gamma^2 W$, when the form of the near edge region becomes controlled by a particular shape of roughnesses, the contribution from the bulk to the average current and the Hall field may dominate and the results of Refs. [28, 29] will describe the observable values.

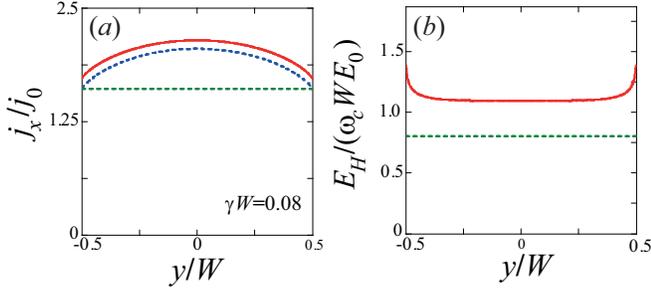


FIG. S2: Current density (a) and Hall field (b) in the bulk part of the sample, $W/2 - |y| \gg \omega_c/\gamma^2$, in the limit $\omega_c \rightarrow 0$ of the first ballistic subregime and at $\gamma W = 0.08$. Red curves present numerical results for $j(y)$ and $E_H(y)$ obtained from integration of the distribution functions (S37), (S40), and (S41). Blue curve in panel (a) correspond to analytical solution (S38), while green curve shows the main contribution to the current density $j = j_\gamma$. Green curve in panel (b) is plotted according to Eq. (S43).

Second, in this subsection we derive the asymptote of the function f_\pm (S20) at $\omega_c \ll \gamma^2 W$ and the corresponding profiles of the current $j(y)$ and the Hall field $E_H(y)$ by the small parameter $\omega_c/(\gamma^2 W)$. It provides the proper form of f_\pm in the bulk region (S35) at any φ and in the near-edge regions (S36) at the velocity angles being not too close to the x direction $|\pi/2 - |\varphi|| \gg \sqrt{\omega_c(W/2 - |y|)}$. The same asymptotic form of f_\pm in the bulk region was obtained in Refs. [28, 29] within the perturbation approach: a direct solution of the kinetic equation in the limits $\gamma W \ll 1$ and $\omega_c W \ll 1$.

In the zeroth order by ω_c , functions f_\pm (S20) take the well-known form [30],[28]:

$$f_{0,\pm}(y, \varphi) = E_0 \frac{\sin \varphi}{\gamma} \left[1 - \exp \left(-\gamma \frac{y \pm W/2}{\cos \varphi} \right) \right], \quad (\text{S37})$$

with the zero coefficients $c_{l,r}$. The flow density corresponding to Eq. (S37) in the leading order by the parameter γW is homogeneous, while an y -dependence emerges in the next order by γW [28]:

$$\begin{aligned} j(y) &= j_\gamma + \Delta j(y), \\ \frac{j_\gamma}{j_0} &= \frac{2}{\pi} \ln \left(\frac{1}{\gamma W} \right), \quad j_0 = \frac{n_0 E_0 W}{m}, \\ \frac{\Delta j(y)}{j_0} &= -\frac{2}{\pi} \left[\left(\frac{1}{2} + \frac{y}{W} \right) \ln \left(\frac{1}{2} + \frac{y}{W} \right) + \right. \\ &\quad \left. + \left(\frac{1}{2} - \frac{y}{W} \right) \ln \left(\frac{1}{2} - \frac{y}{W} \right) \right]. \end{aligned} \quad (\text{S38})$$

The current $\Delta j(y)$ profile has infinite derivatives at the sample edges $y = \pm W/2$ [see Fig. S2(a)].

As it follows from Eq. (S37) the logarithmic divergence in j_γ by γ originates from the electrons whose the velocity angles lie in the diapason: $|\varphi - \pi/2| \lesssim \delta_m(y)$, where

$\delta_m(y) = \gamma(W/2 \pm y) \ll 1$. Such electrons move almost parallel to the sample edges and spend much longer time between scattering in the edges as compared with other electrons having the angles $\varphi \sim 1$. Therefore the first electrons acquire much larger velocity contributions due to acceleration by the electric field E_0 , $v_x(t) = E_0 t$.

Direct calculations yield that the first order term in the expansion of f_\pm (S20) in the powers of ω_c coincides with the function f_1 obtained in Ref. [29] in a perturbation solution of Eq. (S17). Such f_1 satisfies the nontrivial boundary conditions (S4) with $c_{l,r} \neq 0$ and can be written as:

$$f_1 = f_1^z + \delta f_1, \quad (\text{S39})$$

where

$$\begin{aligned} f_1^z(y, \varphi) &= \omega_c E_0 \left\{ \frac{\cos \varphi}{\gamma^2} - \exp \left[-\gamma \frac{y \pm W/2}{\cos \varphi} \right] \right. \\ &\quad \left. \times \left[\frac{\cos \varphi}{\gamma^2} + \frac{y \pm W/2}{\gamma} - \frac{\sin^2 \varphi}{2 \cos^3 \varphi} \left(y \pm \frac{W}{2} \right)^2 \right] \right\} \end{aligned} \quad (\text{S40})$$

is the solution of the inhomogeneous kinetic equation ($E_0 \neq 0$) with zero boundary conditions, while the term

$$\delta f_1(y, \varphi) = \mp \omega_c E_0 \frac{W}{4\gamma} \exp \left(-\gamma \frac{y \pm W/2}{\cos \varphi} \right), \quad (\text{S41})$$

being the solution of the kinetic equation with $E_0 = 0$, ensures that the conditions (S4) are met. The function δf_1 is much smaller than f_1^z at $|\varphi - \pi/2| \lesssim \delta_m$, however δf_1 and f_1^z give comparable contributions to j_y [boundary condition (S4) require that $j_y(y = \pm W/2) = 0$].

Combining of Eqs. (S40), (S41), and (S8), we obtain for the zero harmonic of f_1 :

$$f^{m=0}(y) = -E_0 \frac{\omega_c y W}{\pi} \ln[1/(\gamma W)]. \quad (\text{S42})$$

for the Hall field in the central bulk region (S35) in the leading order by γW [29]:

$$E_H(y) = E_0 \frac{\omega_c W}{\pi} \ln \left(\frac{1}{\gamma W} \right). \quad (\text{S43})$$

The numerically calculated exact profile $E_H(y)$ corresponding to Eqs. (S40) and (S41) differs from this analytical formula (S43) on the values of the order of $E_0 \omega_c W$ [see Fig. S2(b)]. It is noteworthy that the perturbation theory result (S43) is linear by magnetic field, like it takes place for the Hall field in bulk conductors.

Formulas (S38) and (S43) lead to the following expression for the Hall resistance $\varrho_{xy} = E_H/j_\gamma$:

$$\varrho_{xy} = \frac{1}{2} \varrho_{xy}^{(0)}, \quad \varrho_{xy}^{(0)} = \frac{m \omega_c}{n_0} = \frac{B}{n_0 e c}, \quad (\text{S44})$$

where $\varrho_{xy}^{(0)}$ is the conventional Hall resistance for the Ohmic and the hydrodynamic flows of charged particles at low temperatures.

The second-order correction $f_2 \sim \omega_c^2$ to the electron distribution function was calculated in Ref. [28]. At the velocity directions being close to the sample direction, $|\varphi - \pi/2| \ll 1$, the function f_2 in the central region given by Eq. (S35) in the main order by $1/(\gamma W)$ has the form:

$$f_2(y, \varphi) = \frac{\omega_c^2 E}{2 \cos^5 \varphi} \left(y \pm \frac{W}{2}\right)^3 \times \left[1 - \frac{1}{4} \left(y \pm \frac{W}{2}\right) \frac{\gamma}{\cos \varphi}\right] \times \exp\left[-\frac{\gamma}{\cos \varphi} \left(y \pm \frac{W}{2}\right)\right]. \quad (\text{S45})$$

This correction leads to a magnetic field dependence of the current density in the bulk region (S35):

$$j = j_\gamma + j_2, \quad j_2 = \frac{3n_0 E_0}{2\pi m} \frac{\omega_c^2}{W\gamma^4}. \quad (\text{S46})$$

The origin of correction (S47) consists in a small increase of the mean length of the electron collisionless trajectories between the sample edges at nonzero magnetic fields (see Fig. 1 in Ref. [28]).

The obtained positive correction to the current, j_2 (S46), leads to the small negative magnetoresistance of the bulk of the sample:

$$\frac{\varrho_{xx}(B) - \varrho_{xx}(0)}{\varrho_{xx}(0)} = -\frac{3\omega_c^2}{4\gamma^4 W^2 \ln[1/(\gamma W)]}, \quad (\text{S47})$$

where $\varrho_{xx}(0) = E_0/j_\gamma$. It was discussed in Refs. [28, 29] that for not too long samples, $W \ll L \ll 1/\gamma$, the bulk scattering rate γ in this formula is replaced on the reciprocal sample length, $1/L$, and the magnetoresistance (S47) becomes temperature-independent.

Third, we study the flow in the near-edge regions (S36).

In them, one of the components of the distribution function f_\pm (S20), namely, f_+ for $y \approx -W/2$ and f_- for $y \approx W/2$, at the angles close to the sample direction,

$$|\pi/2 - |\varphi|| \lesssim \delta_\pm(y), \quad (\text{S48})$$

$$\delta_\pm(y) = \sqrt{\omega_c(W/2 \pm y)},$$

takes the form of the purely ballistic function (S28), but with the constants $\tilde{c}_{l,r}$ still corresponding to the low-B functions (S41):

$$\tilde{c}_{l,r} = \mp \frac{\omega_c E_0}{4\gamma}. \quad (\text{S49})$$

At the other angles $|\pi/2 - |\varphi|| \gg \delta_\pm(y)$, these components f_\pm coincide with the main parts in formulas (S37), (S39), and (S45) by the parameter γW . The other components of the distribution function, f_+ at $y \approx W/2$ and f_- at $y \approx -W/2$, are still described by the perturbative

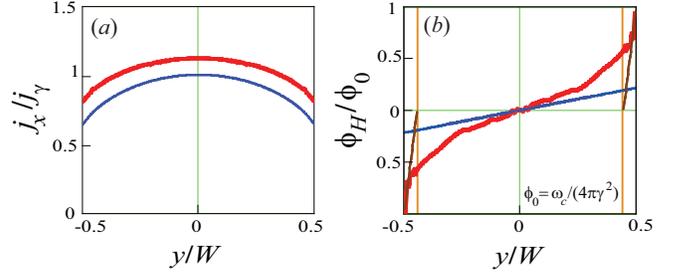


FIG. S3: Current density $j(y)$ (a) and the potential $\phi_H(y)$ of the Hall electric field $E_H(y) = -\phi_H'(y)$ (b) at a finite magnetic field in the first ballistic subregime, $\omega_c \ll \gamma^2 W$, in the whole sample, $|y| < W/2$. The vertical dashed lines depict the boundaries y_b , $W/2 - |y_b| \sim \omega_c/\gamma^2$ of the near-edge regions (S36). The exact values of the flow parameters are: $\omega_c W = 0.01$, $\gamma W = 0.3$. Red curves on both panels present numerical results for $j(y)$ and $E_H(y)$ obtained by general formula (S20). Blue curve on both panels corresponds to the results of the perturbation theory for the bulk region, Eqs. (S38) and (S43). Brown curves on panel (b) are the asymptote non-perturbation formula (S50) for the near edge-regions.

equations (S37)-(S45) at any angles φ in the corresponding domain (S18) or (S19).

In this way, the first form of the distribution functions f_\pm (S34) at the angles $|\pi/2 - |\varphi|| \lesssim \sqrt{\omega_c(W/2 - |y|)}$ is non-perturbative by B and describes the skipping ballistic trajectories.

This result on the form of the function f_\pm (S20) allows us to estimate the corresponding $j(y)$ and $E_H(y)$ in the edge vicinities (S36).

The zero harmonic $f^{m=0}$ of such distribution in the near-edge regions $y \approx \pm W/2$ (S36) is estimated as:

$$f^{m=0}(y) \sim -E_0 \omega_c \left[\pm \frac{1}{\gamma^2} + \frac{y \mp W/2}{\omega_c} \right], \quad (\text{S50})$$

being much larger than its value in the bulk region, Eq. (S42). This result is due to the contribution from the strongly singular term $\sim 1/\cos^3 \varphi$ in Eq. (S40). Such contribution vanishes in the bulk region, where the components f_+ and f_- have the same form (S40) in the whole diapason of φ , that leads to compensation of this contribution from f_+ and f_- . Equation (S50) corresponds to the following estimate of the Hall field (S32) inside the near-edge regions (S36):

$$E_H(y) \sim E_0, \quad W/2 - |y| \lesssim \omega_c/\gamma^2. \quad (\text{S51})$$

Such E_H is the order of the bulk result (S42) at the inner boundaries of these intervals $y \approx \pm(W/2 - \omega_c/\gamma^2)$.

So the Hall electric field $E_H(y)$ is strongly enhanced in the near-edge regions and becomes non-analytical by ω_c [see Eq. (S51) and Fig. S3(b)]. The resulting Hall voltage $U_H = -\int_{-W/2}^{W/2} dy E_H(y)$ turns out to be equal to

$$U_H = -\frac{E_0}{2\pi} \frac{\omega_c}{\gamma^2}, \quad (\text{S52})$$

that correspond to an anomalously large Hall resistance $\varrho_{xy} = U_H/(Wj)$:

$$\varrho_{xy} = \frac{1}{4\gamma^2 W^2 \ln[1/(\gamma W)]} \varrho_{xy}^{(0)}. \quad (\text{S53})$$

Equation (S52) contains exact coefficient as in the very edges, $y = \pm W/2$, only the incident electrons, having the regular first subregime distribution (S39), contribute to the zero harmonic $f^{m=0}(\pm W/2)$ [the first term in Eq. (S50)].

In this way, the anomalous behavior of $E_H(y)$ and ϱ_{xy} originates from the decompensation of the densities of the electrons reflected from one edge in the vicinities of the opposite edge due to the appearance of the skipping electrons which, after the reflection from the last edge, return to it.

For the current density in the near-edge regions (S36) [those can be written as $y = \pm(W/2 - \xi)$, $\xi \lesssim \omega_c/\gamma^2$] we obtain in the main order by γW and $\delta_{\pm}(y)$:

$$j(y) \approx \frac{2j_0}{\pi} \left\{ \left(\frac{1}{2} \mp \frac{y}{W} \right) \ln \left[\frac{1}{\delta_{\pm}(y)} \right] + \left(\frac{1}{2} \pm \frac{y}{W} \right) \ln \left[\frac{1}{\gamma(W/2 \pm y)} \right] \right\}. \quad (\text{S54})$$

The logarithms in both the first and the second term in this formula are estimated as $\ln(\gamma/\omega_c)$ at typical y in the intervals (S36) [see Eq. (S48)]. For the deviation of the current density averaged by the sample width, $j = \int_{-W/2}^{W/2} j(y) dy/W$, from its value in zero magnetic field we obtain from Eqs. (S38) and (S54) in main order by γW and $\delta_{\pm}(y)$:

$$\begin{aligned} j - j_0 - \int_{-W/2}^{W/2} dy \Delta j(y) &\sim \\ &\sim j_0 \int_0^{\omega_c/\gamma^2} d\xi \xi \left\{ \ln \left[\frac{1}{\sqrt{\xi\omega_c}} \right] - \ln \left[\frac{1}{\xi\gamma} \right] \right\} \sim \\ &\sim -j_0 \frac{\omega_c^2}{\gamma^4 W^2} \ln \left(\frac{\gamma}{\omega_c} \right). \end{aligned} \quad (\text{S55})$$

This correction to the current leads to a positive nonanalytical magnetoresistance:

$$\frac{\varrho_{xx}(B) - \varrho_{xx}(0)}{\varrho_{xx}(0)} = \frac{\omega_c^2 \ln(\gamma/\omega_c)}{\gamma^4 W^2 \ln[1/(\gamma W)]}, \quad (\text{S56})$$

Such magnetoresistance accounts the difference of the contributions of the near-edge regions to the current density as compared with the bulk one: the boundary $\delta_m(y) = \gamma(W/2 - y)$ for the angles of the electrons giving the main contribution to $j(y)$ in the bulk region (S35) is changed on the values $\delta_{\pm}(y) \gg \delta_m(y)$ (S48) for a half of electrons in the near-edge regions (those are the skipping electrons).

In real samples, depending on their geometry both the bulk and the edge contributions to magnetoresistance and the Hall effect corresponding to Eqs. (S43), (S47) or (S52), (S56) may appear. For long samples of very high quality, where the described above skipping trajectories are realized near the longitudinal edges, the observed values of $\varrho_{xx}(B)$ and $\varrho_{xy}(B)$ will be determined by the near-edge regions, as their contributions to the magnetic field-dependent values are greater than the bulk contributions. For samples of more irregular geometry (not so long and straight), the contribution from the near-edge regions can be, apparently, suppressed, thus the bulk magnetoresistance (S47) and Hall effect (S43) may manifest themselves in the observed $\varrho_{xx}(B)$ and $\varrho_{xy}(B)$.

We note that even in long straight stripes, the position of the Hall contacts can strongly influence the manifestation of the bulk or the near-edge Hall resistance.

Fourth, we present in this subsection an elementary derivation of the result of Ref. [29] equations (S38), (S43), and (S44) not employing the kinetic equation. It seems that such derivation explains, to some extent, why the Hall resistance of the central part of the ballistic samples in the limit $\omega_c \rightarrow 0$ is equal to one half of the conventional Hall resistance of macroscopic Ohmic samples, $\varrho_{xy}^0 = B/(n_0 e c)$.

Formulas (S38), (S43), and (S46), for the integral values characterizing the flow in the bulk region (S35) in the limit $\omega_c \rightarrow 0$ were derived from the kinetic equation (S17) taking into account only the departure term $-\gamma f$ in the collision integral and the magnetic field term $\omega_c \partial f / \partial \varphi$. This implies that the particles that after an edge-scattering event reach the other edge without inter-particle collisions (at the velocity angles $|\varphi| - \pi/2 \gg \delta_m$) or undergo an inter-particle collision (at $|\varphi| - \pi/2 \lesssim \delta_m$) in the bulk. Herewith the main contribution to the current and the Hall field comes from the electrons with the velocity angles $\delta_m \lesssim |\pi/2 - |\varphi|| \ll 1$. The Hall electric field is mainly determined by the requirement of the balance of the Lorentz force and the Hall field acting on the same ballistic electrons with the angles $\delta_m \lesssim |\varphi| - \pi/2 \ll 1$.

In the limit of very weak external fields, $\omega_c \rightarrow 0$ and $E_0 \rightarrow 0$, electron trajectories $\mathbf{r}(t) = [x(t), y(t)]$ are almost straight lines. For example, for the x component of the velocity $\mathbf{v} = \dot{\mathbf{r}}$ of an electron reflected by the angle φ from the left edge we have:

$$v_x(t, \varphi) = v_F \sin \varphi + \frac{eE_0}{m} t, \quad (\text{S57})$$

where the time t is counted from the moment of the last reflection of this electron from the edge. In Eqs. (S57) and until the end of this subsection we again write the Fermi velocity v_F explicitly for better comprehension of the text.

The mean current density j is calculated by the Drude

formula:

$$j = n_0 t_0 E_0 / m, \quad (\text{S58})$$

where t_0 is the mean time of a free motion of electrons in the bulk. In the first ballistic regime, the value t_0 is obtained by the proper averaging of the times $t_{\pm}(y = \pm W/2, \varphi)$ of collisionless motion of individual electrons between the edges. Here the value $t_{\pm}(y, \varphi)$ corresponds to the electron trajectories between the edge $y = \mp W/2$ and the point y , unperturbed by external field:

$$t_{\pm}(y, \varphi) = \frac{W/2 \pm y}{v_F |\cos \varphi|}. \quad (\text{S59})$$

In order to find t_0 , one needs to integrate $t_{\pm}(y = \pm W/2, \varphi)$ by φ up to the limiting values of $\varphi = \varphi_m \approx \pm \pi/2$ at which $|\pi/2 - |\varphi||$ is equal to $\delta_m \sim \gamma W$. Such limits correspond to the ballistic trajectories with the maximum length equal to the mean free path relative to the bulk scattering, $l = 1/\gamma$. After the integration, we obtain $j = j_{\gamma}$ for the mean current density, where j_{γ} is defined in Eq. (S38).

Next, we calculate the Hall field E_H in the bulk within similar approach. We suppose E_H to be homogeneous in y , $E_H(y) \approx E_H$, that is, we exclude the near-edge regions from this consideration. In order to find E_H , we use the y component of Newton's equations having the form:

$$m\dot{v}_y = eE_H + \frac{eB}{c} v_x. \quad (\text{S60})$$

After the averaging of this equation by φ at a given y , only the contribution to v_x related to the acceleration by the field E_0 [see Eq. (S57)] remains non-zero at any y . This fact and Eq. (S60) leads to the estimates $\dot{v}_y \sim E_0 B$ and $E_H \sim E_0 B$ in the limit $E_0, B \rightarrow 0$. Next, due to the sample edges, there is no acceleration along the y direction of the whole ensemble of electrons in the sample,

$$\sum_{\pm} \int_0^{2\pi} \frac{d\varphi}{2\pi} \int_{-W/2}^{W/2} \frac{dy}{W} m\dot{v}_y[t_{\pm}(y, \varphi), \varphi] = 0, \quad (\text{S61})$$

where the vicinities of the angles $\pm \pi/2$ of the size γW are excluded in the integral by $d\varphi$. Equation (S60) averaged over all electrons in the samples [integrated by $d\varphi$ and dy with the same restriction $||\varphi - \pi/2| \lesssim \gamma W$] together with condition (S61):

$$0 = E_H + \frac{B}{c} \sum_{\pm} \int_0^{2\pi} \frac{d\varphi}{2\pi} \int_{-W/2}^{W/2} \frac{dy}{W} v_x[t_{\pm}(y, \varphi), \varphi], \quad (\text{S62})$$

yields result (S43) for the Hall electric field E_H .

In view of the above elementary consideration, it becomes apparent that the factor 1/2 in Eq. (S44) has a kinematic origin. Indeed, the value of E_H following from

the condition (S62) of compensation of the linearly increasing in time magnetic Lorenz force by the force from the Hall electric field, contains the mean time of free motion t_0 and the factor 1/2 [see Eqs. (S57), (S59), and (S62)]. Expression (S58) for the mean current density j contains the same time t_0 and the dimensional factors with no numeric factors. Thus the ratio of E_H and j acquires additional factor 1/2 as compared with the case of the Ohmic and hydrodynamic regime, when both E_H and j are calculated from the other averaging procedure based on the local hydrodynamic velocity $V_x(y) = j(y)/[n/m]$ and the condition $V_y \equiv 0$ instead of Eq. (S61) in the ballistic flow.

3. MEAN FIELD SOLUTION IN VICINITY OF PHASE TRANSITION

3.1. Ballistic solution near critical field

Our approach allows one to consider the systems being the mixtures of the two cases: (i) there are no bulk defects and the electrons inside the sample are scattered only on each other, conserving momentum; or (ii) there are no inter-particle collisions, but inside the sample the scattering of electrons by a weak disorder, leading to a weak momentum relaxation, takes place. For simplicity, we consider only such two marginal types of samples in which only one of the scattering mechanisms acts: the electron-electron collisions ($\gamma_d = 0$, $\gamma = \gamma_{ee}$) or the scattering on disorder ($\gamma_{ee} = 0$, $\gamma = \gamma_d$).

In this subsection, from the general ballistic solution (S20), we obtain the simplified distribution function in the low vicinity, $0 < 2 - \omega_c W \ll 1$, of the critical magnetic field $\omega_c^{cr} = 2/W$, taking into account the departure term $-\gamma f$ of the bulk scattering in the kinetic equation. Such solution provides a full description of the transport at $\omega_c W < 2$ in the disordered samples with no electron-electron scattering, that is of the low vicinity of the ballistic-Ohmic phase transition. It is also a basis element for the derivation of the distribution at $\omega_c W < 2$ in pure samples with only electron-electron collisions (the low vicinity of the ballistic-hydrodynamic phase transition).

The coefficients I_{ll} , I_{lr} of the system of linear equations (S23) tend to zero at $2 - \omega_c W \ll 1$. From Eqs. (S24) and (S25) for I_{ll} , I_{lr} in main order by the small parameters $2 - \omega_c W \ll 1$ and $\gamma/\omega_c \ll 1$ we have:

$$I_{ll} = 2 - \omega_c W + \frac{2\pi\gamma}{\omega_c}, \quad I_{lr} = 2 - \omega_c W. \quad (\text{S63})$$

Herewith, it follows from Eq. (S26) that the right-hand side coefficients in Eq. (S23) remains finite:

$$I_l = -\pi\omega. \quad (\text{S64})$$

From Eqs. (S23), (S63), and (S64) we obtain that the parameters c_{\pm} in distribution function (S20) takes the form:

$$c_{\pm} = \pm \frac{\omega_c/2}{\gamma/\omega_c + (2 - \omega_c W)/\pi}. \quad (\text{S65})$$

We see that such c_{\pm} have a divergent behavior at $\omega_c \rightarrow \omega_c^{cr}$, becoming much larger than unity, while other terms in general solution g_{\pm} (S20) do not exhibit a divergence at $\omega_c \rightarrow \omega_c^{cr}$. In this regard, the distribution function (S20) in the main order by the small parameters $2 - \omega_c W$ and γW is given by:

$$f_{\pm}(y, \varphi) = \frac{E_0}{\omega_c^2} c_{\pm}. \quad (\text{S66})$$

Such distribution function is a generalization of the fully ballistic solution (S33). The last one is valid not in the very vicinity ω_c^{cr} , $\gamma W \ll 2 - \omega_c W \ll 1$, as in that any bulk scattering is neglected.

The function f_{\pm} (S66) describes a redistribution of electrons between the left and the right regions (S18) and (S19) [see Fig. S1], being homogeneous in each region. At $2 - W/R_c \ll 1$, the most of inequilibrium electrons described by f_{\pm} (S66) are the skipping electrons, those after the reflection from an edge returns to the same edge. Only a very small fraction of reflected electrons reaches the opposite edge [see Fig. S1 and Fig. 1(b) in the main text].

The $\mathbf{E} \times \mathbf{B}$ -drift flow in the y direction, described by the space-homogeneous Drude part of the distribution function (S20), is compensated only by the electrons reaching the opposite edge, as each skipping electron provide no contribution to the flow in the y direction. The density of the inequilibrium electrons reaching the opposite edge is proportional to the coefficients c_{\pm} times the small relative part of such electrons. This explains why the coefficients c_{\pm} at $\omega_c W \rightarrow 2$ must be very large.

Beside this, there is a small part of the skipping electrons, which would have returned to the same edge, but, due to an electron-electron collision, will not actually return. Such electrons leads to an additional compensation of the $\mathbf{E} \times \mathbf{B}$ drift flow and, thus, weakens the imbalance between the electrons in the left and right regions. That is why the divergence of c_{\pm} at $\omega_c W \rightarrow 2$ is limited by the scattering rate γ in Eq. (S65).

The current density and the Hall electric field for distribution function (S66) in the main order by γ and ε takes the forms:

$$j(y) = \frac{2nE_0}{\pi m} \frac{1}{\gamma + \varepsilon} \sqrt{1 - \omega_c^2 y^2} \quad (\text{S67})$$

and

$$E_H(y) = \frac{E_0}{\pi} \frac{1}{\gamma + \varepsilon} \frac{\omega_c}{\sqrt{1 - \omega_c^2 y^2}}, \quad (\text{S68})$$

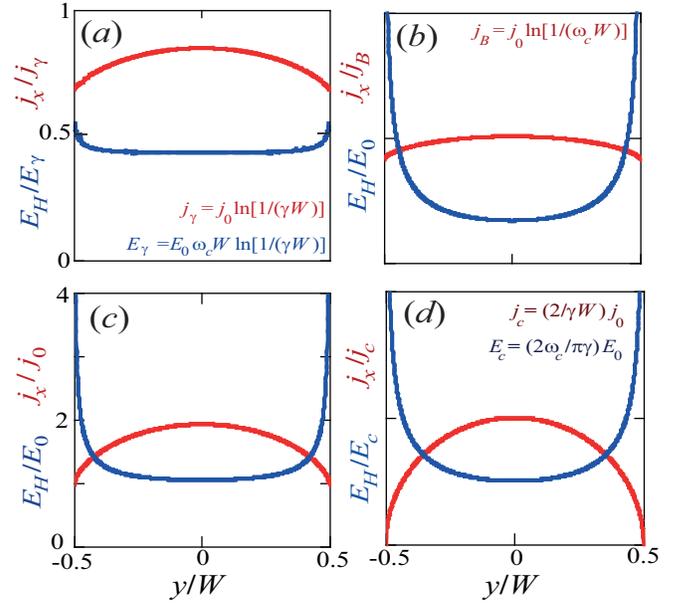


FIG. S4: Profiles of the current density (red curves) and the Hall electric field (blue curves) at different values of magnetic field: (a) the first ballistic subregime in the limit $\omega_c \rightarrow 0$ for the ballistic parameter $\gamma W = 0.08$ (only the bulk of the sample is shown); (b) the second ballistic subregime, corresponding to the small parameter $\omega_c W$, $\omega_c W = 10^{-3}$ [herewith $\omega_c W \gg (\gamma W)^2$]; (c) the third ballistic subregime at the intermediate parameter $\omega_c W$, $\omega_c W = 1$; and (d) the very point of the phase transition, when $\omega_c W = 2$. Curves are plotted by Eqs. (S7) and (S8) with distribution function (S37), (S40), (S41) for (a); with function (S28) for (b) and (c); and by equations (S65), (S66), and (S76) for (d).

where the parameter ε characterizes the proximity to the transition point:

$$\varepsilon = \frac{2 - \omega_c W}{\pi} \omega_c \quad (\text{S69})$$

These profiles correspond to the following averaged values of the current density $j = \int_{-W/2}^{W/2} dy j(y)/W$ and the mean Hall field $E_H = \int_{-W/2}^{W/2} dy E_H(y)/W$:

$$j = \frac{n_0 E_0}{m} \frac{1}{2(\gamma + \varepsilon)} \quad (\text{S70})$$

and

$$E_H = E_0 \frac{\omega_c}{2(\gamma + \varepsilon)}. \quad (\text{S71})$$

Functions (S67) and (S68) as well as the profiles $j(y)$ and $E_H(y)$ in the three ballistic subregimes are plotted in Fig. S4.

It is of importance to perform a more precise calculation of the current density j and the Hall electric field E_H for the critical distribution function (S66). In the next order by the small parameter $\sqrt{\varepsilon}$ we obtain the

same equation (S70) for the mean current density, but the other result for the Hall field:

$$E_H = E_0 \frac{\omega_c}{2(\gamma + \varepsilon)} F(\varepsilon), \quad F(\varepsilon) = 1 - \sqrt{\frac{2}{\pi}} \varepsilon. \quad (\text{S72})$$

Here the factor $F(\varepsilon)$ describes the correction to Eq. (S71) related to deviations of the shapes of the left and the right ballistic regions from their limiting form at $\varepsilon = 0$ [see Fig. S1(b)]. So equations (S70) and (S72) describe the current and the Hall field near the transition in the two first orders by the parameter $\sqrt{\varepsilon}$ and in the main order by the parameter γ .

For brevity, below we omit the factor n_0/m in all current densities. That is, we change the units of the current densities according to: $j \rightarrow j/[n_0/m]$.

It is noteworthy that the obtained values of the ballistic current (S70) and the Hall field (S71) at the transition point $\omega_c W = 2$ turn out to be one half as compared with those obtained within the Drude model for a bulk sample of the same width with the rate γ of the scattering on disorder. Thus, for disordered samples with no interparticle collisions the diffusive scattering on the rough edges and the scattering on the bulk disorder provide the same additive contributions to the total momentum relaxation rate 2γ , appearing in current (S70) and Hall field (S71).

3.2. Mean field theory below critical field

In the case of interacting electrons in the absence of disorder, in the nearest vicinity of the critical magnetic field,

$$0 < 2 - \omega_c W \lesssim \gamma/W, \quad (\text{S73})$$

substitution of the singular distribution function f_{\pm} (S66) into the departure and the arrival terms, γf and $\gamma \hat{P}[f]$, leads to the values of the same order of magnitude as the external field term, $\sim E_0 \sin \varphi$. This indicates that both the terms γf and $\gamma \hat{P}[f]$ are equally important in the region near the transition.

Our approach to the description of the dynamic in interval (S73) is based on taking into account the arrival term $\gamma \hat{P}[f]$ in the way analogous to the mean field theory for thermodynamic phase transitions. Namely, we treat the part of the term $\gamma \hat{P}[f]$ proportional to $\sin \varphi$:

$$\gamma \hat{P}_{\sin}[f](y, \varphi) = \gamma j(y) \sin \varphi, \quad (\text{S74})$$

as an addition ‘‘internal’’ electric field [compare Eqs. (S7) and (S9)]. Herewith we omit its dependence on the coordinate y replacing the factor $j(y)$ in Eq. (S74) by its average value $j = \int_{-W/2}^{W/2} dy j(y)/W$.

It was shown in Refs. [28, 29] that, in the first ballistic subregime, $\omega_c \ll \gamma^2/W$, where $j(y)$ is close to j_{γ} [see Eq. (S38)], this approach is exact in the main order by

the large logarithmic parameter $\ln[1/(\gamma W)]$. In those papers, the corrections to the current and the Hall field from the the arrival term $\gamma \hat{P}[f]$, being small by the parameter $\gamma W \ln[1/(\gamma W)]$, were calculated. Near the transition, the ballistic current density $j(y)$ (S67) is strongly inhomogeneous and, thus, such approach based on the approximate homogeneity of the term $\gamma \hat{P}[f]$ is not exact. However, in accordance with the practice of applying the mean field approximation in thermodynamic phase transition, it is reasonable to believe that such mean field approach will provide a qualitatively correct description of the phase transition.

Let us note that replacing of the arrival term $\gamma \hat{P}[f]$ by its value average by y can be interpreted as using of a special, nonlocal by y , collision integral:

$$\text{St}'[f](y, \varphi) = -\gamma \left\{ f(y, \varphi) - \int_{-W/2}^{W/2} \frac{d\xi}{W} \hat{P}[f](\xi, \varphi) \right\}. \quad (\text{S75})$$

Such collision integral conserves momentum and number of electrons only within the whole sample, but not at a given point y . In this regard, the solution of the kinetic equation with Eq. (S75) leads to a small non-physical current $j_y(y)$ and a small symmetrical part of the density perturbation, $\delta n(y) = \delta n(-y)$, both being proportional to the small parameter γW . Note also that the general solution (S20) of the kinetic equation with the omitted term $\gamma \hat{P}[f]$ also lead to a small non-physical $j_y(y)$, which are much smaller than $j(y)$, and a small symmetrical part of $\delta n(y)$, not leading to any nonzero mean Hall field.

In this way, the self-consistent mean field equation for description of the behavior of the value $j = j(\varepsilon)$, determining the state of the system at different $\varepsilon = \varepsilon(\omega_c)$, is constructed by the substitution:

$$E_0 \rightarrow E_0 + \gamma j \quad (\text{S76})$$

in the ballistic equation (S70) for j . After such substitution, we obtain the self-consistent equation for the current in the transition mixed ballistic-hydrodynamic region (S73):

$$j = \frac{E_0 + \gamma j}{2(\gamma + \varepsilon)}. \quad (\text{S77})$$

Solution of this equation yields:

$$j = \frac{E_0}{\gamma + 2\varepsilon}. \quad (\text{S78})$$

In the very transition point, $\varepsilon = 0$, this value is twice as large compared with the fully ballistic result (S70), neglecting the arrival term $\gamma \hat{P}[f]$.

Result (S78) implies the following electron dynamics. The near-transition distribution function (S66) describe a shortage of the skipping electrons near one of the edge (as compared with the equilibrium state) and the excess

near the other one. The magnitudes of these shortage and excess corresponds to compensation of the $\mathbf{E} \times \mathbf{B}$ -drift along the y direction [the first term in Eq. (S20)]. The compensation of the $\mathbf{E} \times \mathbf{B}$ -drift occurs by the two additive mechanisms: moving of electrons by trajectories connecting opposite edges and scattering in the bulk (on other electrons or on disorder). These two mechanisms correspond to the two terms in denominators of Eqs. (S65), (S70), and (S78): $\sim \varepsilon$ and $\sim \gamma$. Herewith, each scattering of an electron on disorder in the bulk leads to damping of the current carried by it, while each collision of two electrons leads only to change of their trajectories leading to some effective rotation of the currents carried by these two electrons. Thus the scattering on the bulk disorder is (twice) more effective in the purely ballistic solution (S70) [applicable for disordered samples] than the electron-electron scattering in the mean field solution (S78) [applicable for pure hydrodynamic samples].

The Hall electric field with taking into account the arrival term is calculated by the same replacement $E_0 \rightarrow E_0 + \gamma j$ in equation (S72) for the ballistic Hall field taking into account only the departure term. We emphasize that equation (S72), unlike Eqs. (S70) and (S77), does not participate in the self-consistent procedure of determining the state of the system. Using mean field current (S78), we obtain:

$$E_H = (E_0 + \gamma j) \frac{\omega_c}{2(\gamma + \varepsilon)} F(\varepsilon) \quad (\text{S79})$$

from Eqs. (S72) and (S76), that leads to:

$$E_H = E_0 \frac{\omega_c}{\gamma + 2\varepsilon} F(\varepsilon). \quad (\text{S80})$$

Due to the factor $F(\varepsilon)$, this function has a strong square-root singularity at $\omega_c W \rightarrow 2$.

3.3. Mean field theory above critical field

In samples wider than the twice cyclotron radius, $W > 2R_c$, there arises a group of the electrons whose trajectories do not cross the sample edges [see Fig. S1(c) and Fig. 1(c) in the main text]. Such “central” electrons spend a long time, $\sim 1/\gamma \gg W$ on their trajectories without collisions.

It is reasonable to expect that the appearance the central electrons dramatically changes the transport regime. Below we show that the ballistic-hydrodynamic or the ballistic-Ohmic phase transitions occur in pure and in disordered samples, where the electron-electron scattering or the scattering on disorder dominate, respectively. The relative density of the central electrons,

$$\alpha_c = (W - 2R_c)/W = 1 - 2/\omega_c, \quad (\text{S81})$$

can be considered as the order parameter of these transitions. The fraction of the other “edge” electrons those

are scattered mainly on the edges is equal to:

$$\alpha_e = 2R_c/W = 1 - \alpha_c. \quad (\text{S82})$$

The distribution functions f_e and f_c of the edge electrons (“e”) and of the central electrons (“c”) are defined in the two distinct regions in the (y, φ) plane [see Fig. S1(c)]. To describe the transitions, one should solve the exact kinetic equation (S9) in such regions with accounting of both the arrival and the departure terms. The dynamics of the edge electrons is similar to the dynamics of the skipping electrons in the nearest low vicinity (S73) of the phase transition.

In order to describe the central electrons, it is convenient to change the variables y, φ on the new variables y_c, φ , where y_c is the coordinate of the center of electron cyclotron orbits. The positions of the central electrons are drawn by red region in Fig. 1S(c), which is characterized in the new variables by the inequality:

$$-W/2 + R_c < y_c < W/2 - R_c, \quad 0 < \varphi < 2\pi. \quad (\text{S83})$$

For the edge electrons we have:

$$|y_c| > W/2 - R_c, \quad (\text{S84})$$

while their velocity angle φ lies in the diapasons depending on y_c . The solution $f_c(y, \varphi)$ of the exact kinetic equation (S9) with the non-local arrival term $\gamma \hat{P}[f_e + f_c]$ (or $\gamma \hat{P}_0[f_e + f_c]$), mixing the functions f_e and f_c , is a continuous function in diapason (S83). Therefore the angular harmonics $f_{c,m} \sim \int d\varphi f_c(y_c, \varphi) e^{-im\varphi}$ of f_c rapidly decrease with the increase of m (apparently, as a geometric progression). On the contrary, the studied above ballistic solution f_{\pm} (S20) of the truncated kinetic equation (S17), describing the electrons just reflected from edges, has discontinuities at the marginal trajectories shown in Figs. 1(a,b). Thus functions f_{\pm} (S20) has angular harmonic depending on m slowly (as a power of m). So the central electrons are described by a distribution function of a hydrodynamic type and should be considered as a nucleus of the viscous or the Ohmic flow.

Instead of an exact solution of the kinetic equation, we propose a two-component mean field model which is similar to the (one-component) mean field model used in the previous section for the lower vicinity the transition point, $0 < 2 - \omega_c W \ll 1$, and accounting both the central and the edge electrons in a simplified way. Our model is qualitatively applicable, as we believe, in the nearest upper vicinity of the phase transition:

$$0 < \omega_c W - 2 \ll 1. \quad (\text{S85})$$

The exact form of the two-component model is different for the pure and the disordered samples.

First, we study the ballistic-hydrodynamic transition in pure samples when only the electron-electron scattering takes place.

When the fraction of the central electrons is small, $\alpha_c \ll 1$, the centers of their cyclotron orbits lie approximately in the center of the sample, $y = 0$ [see Eq. (S83) and Fig. 1(c) in the main text]. Herewith each central electrons most often scatter on the edge electrons, which have the distribution $f_e(y_c, \varphi)$ varying by y_c on the scale of the order W . Thus the properties of all central electrons in the main order by γ and α_c are almost identical and are described by the distribution function f_c weakly depending on y :

$$f_c(y_c, \varphi) \approx f_c(0, \varphi). \quad (\text{S86})$$

Within the mean-field approach that we develop, we use only one parameter to describe the state of the central electrons. It is their contribution to the averaged current density, j_c , related to f_c (S86). Herewith, for the description of the state of the edge electrons we also use the similar mean field parameter, j_e , being the other contribution to the averaged current.

To find j_e we note that the ballistic kinetic equation (S17) with the arrival term simplified according to Eqs. (S75) and (S76) and boundary conditions (S4) is still applicable in the main order by $\gamma \ll \omega_c$ and $\alpha_c \ll 1$ for the edge electrons at their regions on the (y, φ) -plane [see Fig. 1S(c)]. Thus, in the main order by the parameter γ , the solution f_{\pm} (S66) at $\varepsilon = 0$ with the proper effective field:

$$E_0 \rightarrow E_0 + \gamma(j_e + j_c), \quad (\text{S87})$$

remains valid also for the edge electrons in the nearest upper vicinity of the transition. Integration of function f_{\pm} (S66) of the edge electrons with the factor $\sin \varphi$ over the left and the right edge regions (see Fig. S1) yields in the main order by α_c and γ similar formulas for the edge contributions to j and E_H at the effective field $E + \gamma j$ (S87) as the integration of f_{\pm} (S66) at the critical magnetic field $\omega_c = 2/W$ over the whole sample:

$$j_e = \alpha_e \frac{E_0 + \gamma(j_e + j_c)}{2\gamma}, \quad (\text{S88})$$

where the factor α_e takes into account the relative edge electron density [compare Eqs. (S88) and (S77)].

In order to calculate j_c , we multiply the kinetic equation (S9) expressed in the variables φ, y_c on the factor $\sin \varphi$ and integrate it by φ and y_c over $-\pi/2 < \varphi < 3\pi/2$ and $-W/2 + R_c < y_c < W/2 - R_c$. In this diapason of y_c , the distribution function f_c describes the central electrons and is approximately independent on y_c , according to Eq. (S86). As the result, we arrive to the formula:

$$j_c = \alpha_c \frac{E_0 + \gamma(j_e + j_c)}{\gamma}. \quad (\text{S89})$$

This is actually the Drude formula for the contribution to the total current from central electrons, which are scattered on the edge electrons with the rate γ and accelerated by the effective field (S87).

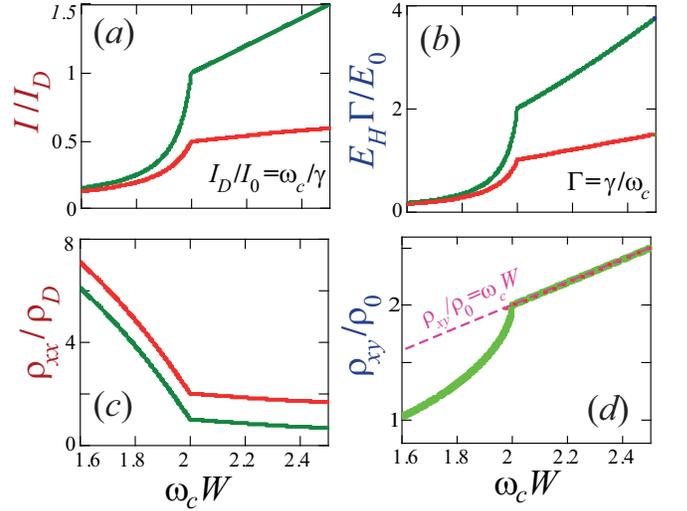


FIG. S5: Current (a), Hall electric field (b), longitudinal (c) and Hall (d) resistances as functions of magnetic field in a wide region around the critical field, $\omega_c W = 2$, for the ballistic-hydrodynamic phase transition [green curves] and for the ballistic-Ohmic phase transition [red curves]. In panel (d) for the Hall resistances, the green and the red curves, corresponding to the both types of the transitions, coincide.

Solving together the resulting system of mean field equations (S88) and (S89) and keeping in mind that $\alpha_e + \alpha_c = 1$, we obtain in the main order by γ :

$$j_e = \frac{E_0}{\gamma}, \quad j_c = 2\alpha_c \frac{E_0}{\gamma}. \quad (\text{S90})$$

For the total current we obtain from Eq. (S90):

$$j = (1 + 2\alpha_c) \frac{E_0}{\gamma}. \quad (\text{S91})$$

According to the definition of α_c , this function grows linearly with the difference $B - B_c$ [see Fig. S5(a)].

The physical picture implied under the second equation in formulas (S90) is as follows. The dynamics of the central electrons in the reference frame moving with the drift velocity of the edge electrons is similar to the scattering on static defects. Namely, the edge electrons are looked like static defects for the central electrons in this moving frame. The effective momentum relaxation time of the edge electrons due scattering on the edges and on other edge electrons is exactly $1/\gamma$ [see the first equation in formula (S90)]. The time of the (electron-electron) scattering of the central electrons on the edge electrons is also equal to $1/\gamma$. As the actual mean velocity of the central electrons is the sum of and their mean velocity in the moving frame and the velocity of the frame $v_e^{dr} = E_0/\gamma$, a doubling of the scattering time $1/\gamma$ in equation for j_c in Eqs. (S90) arises.

The Hall electric field above the transition also contains the contributions from the edge electrons and from

the central ones. As the ballistic solution f_{\pm} (S66) with the effective field (S87) remains approximately valid for the edge electrons at $0 < \omega_c W - 2 \ll 1$, the edge electrons contribution to the Hall field in the main order by γ is described by equation (S79). In it, we should put $\varepsilon = 0$, use Eq. (S91) for the current j , and introduce the factor α_e accounting the relative density of the edge electrons. We obtain:

$$E_{H,e} = \alpha_e (1 + \alpha_c) \frac{\omega_c}{\gamma} E_0, \quad (\text{S92})$$

that is equal to $\omega_c E_0 / \gamma$ in the zero and the first orders by $\alpha_c \ll 1$.

The contribution to the Hall field from the central electrons is calculated using the y -independent distribution function $f_c(y_c, \varphi) \approx f_c(0, \varphi)$. Multiplying kinetic equation (S9) on $\cos \varphi$ and integrating over $-\pi/2 < \varphi < 3\pi/2$ and $-W/2 + R_c < y_c < W/2 - R_c$, we obtain the contribution to the Hall field, similar to the result in the Drude theory:

$$E_{H,c} = \omega_c j_c. \quad (\text{S93})$$

From Eq. (S90) we get that the averaged Hall field consisting of the contributions (S92) and (S93) takes the form:

$$E_H = (1 + 2\alpha_c) \frac{\omega_c}{\gamma} E_0. \quad (\text{S94})$$

The functions $j(\omega_c)$ (S91) and $E_H(\omega_c)$ (S94), together with the corresponding resistances $\varrho_{xx}(\omega_c) = E_0/j$ and $\varrho_{xy}(\omega_c) = E_H/j$, are plotted in Figs. S5 and S6.

Second, let us consider the ballistic-Ohmic phase transition in a sample in which only scattering on disorder in the bulk is substantial.

In such system, the contribution to the current from the edge and from the central electrons are independent. For the contributions to j and E_H from edge electrons one should use just the pure ballistic formulas (S70) and (S71) at $\varepsilon = 0$, multiplied on the fraction of the edge electrons α_e :

$$j_e = \alpha_e \frac{E_0}{2\gamma}, \quad E_{H,e} = \alpha_e \frac{\omega_c}{2\gamma} E_0. \quad (\text{S95})$$

For the contribution to the current and the Hall field from the central electrons we should use the Drude formulas with the factor α_c accounting their relative density:

$$j_c = \alpha_c \frac{E_0}{\gamma}, \quad E_{H,c} = \alpha_c \frac{\omega_c E_0}{\gamma}. \quad (\text{S96})$$

Keeping in mind that $\alpha_c + \alpha_e = 1$, for the mean current density and the Hall field we obtain:

$$j = \frac{1 + \alpha_c}{2} \frac{E_0}{\gamma}, \quad E_H = \frac{1 + \alpha_c}{2} \frac{\omega_c E_0}{\gamma}. \quad (\text{S97})$$

Unlike the pure samples where only the electron-electron scattering takes place in the bulk, results (S97) remains

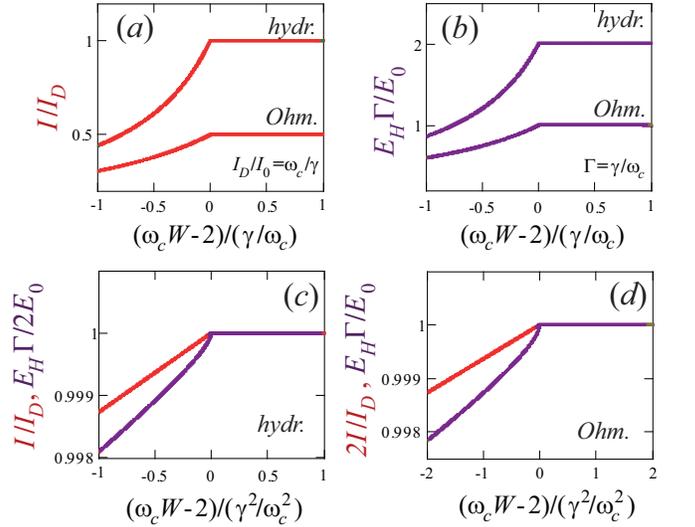


FIG. S6: Current (red lines) and Hall electric field (purple lines) as functions of magnetic field in narrow (a,b) and in very narrow (c,d) vicinities of the critical point $\omega_c W = 2$ for the ballistic-hydrodynamic and for the ballistic-Ohmic phase transition (see the captions on curves and on panels).

valid in the disordered samples at any relation between the fractions α_c and α_e of electrons of the both groups. In particular, in the limit of very large fields, when $W \gg R_c$ and $\alpha_c \approx 1$, equations (S97) turn into the usual Drude formulas for long Ohmic samples.

From the obtained results we see that, in both the ballistic-hydrodynamic and the ballistic-Ohmic phase transitions, the dependence of the current on magnetic field, $j(\omega_c)$, has a jump of its derivative (a kink) at the critical field $\omega_c^{cr} = 2/W$, while the Hall field $E_H(\omega_c)$ has even a square root singularity at $\omega_c \rightarrow \omega_c^{cr} - 0$ (see Figs. S5 and S6).

Of particular interest is the behavior of the Hall resistance $\varrho_{xy} = E_H/j$. First, it is seen that the dependence $\varrho_{xy}(\omega_c)$ for both the ballistic-hydrodynamic and ballistic-Ohmic transitions coincide one with another [see Fig. S5(d)]. Second, above the transition point, $\omega_c > \omega_c^{cr}$, the function $\varrho_{xy}(\omega_c)$ is identically equal to its “standard” value $\varrho_{xy}^0 = B/n_0 e c$, corresponding to the usual Ohmic regime at low temperatures.

On the contrary, the behavior of the current and the corresponding longitudinal resistance near the transition field are quite different for the two phase transitions (see Figs. S5(a,c)).

Third, we briefly discuss the behavior of the central electron far beyond the transition, when $W - 2R_c \sim W$ or $W - 2R_c \approx W \gg R_c$. In this case the fraction of the central electrons is comparable or greater than the one of the edge electrons: $\alpha_c \sim \alpha_e \sim 1$ or $\alpha_c \approx 1$, $\alpha_e \ll 1$. The collisions between the central becomes important. The central electrons located farther from the edges are less likely to collide with edge electrons than central electrons

located closer to the edge. This inhomogeneity of scattering leads to the the formation of an inhomogeneous, parabolic by y , profile $j(y)$ of the Poiseuille flow.

The region $W/R_c - 2 \gtrsim 1$ for the ballistic-hydrodynamic phase transition was studied by the numeric solution of the kinetic equation in Refs. [25],[26]. As it was just mentioned, above formulas (S97) for j and E_H in the ballistic-Ohmic transition are valid at any relation between R_c and W .

In pure hydrodynamic samples, at large magnetic fields, $\omega_c \gg 1/W$, the hydrodynamic contribution from the central electrons to the current dominates to the averaged resistance is given by the formula [19]:

$$\varrho_P = \frac{12\eta_{xx}}{W^2}, \quad (\text{S98})$$

where η_{xx} is the diagonal viscosity coefficient, being equal in our notations to $\eta_{xx} = \gamma/(16\omega_c^2)$ at $\gamma \ll \omega_c$. Thus, we obtain for the averaged sample resistance at $W \gg 1/\omega_c$:

$$\varrho_P(\omega_c) = \frac{3}{4} \frac{\gamma}{\omega_c^2 W^2}. \quad (\text{S99})$$

In this formula the contribution from the edge electrons is neglected.

For disordered samples, we obtain from Ref. (S97) in the limit $W \gg R_c$ the Drude result for magnetoresistance, being independent on ω_c :

$$\varrho_D(\omega_c) = \gamma. \quad (\text{S100})$$

In the usual units, this is the conventional Drude formula $m\gamma/(n_0e^2)$.

It is noteworthy that both resistances (S99) and (S100) are proportional to the scattering rate γ , but the second one decreases with the magnetic field as $\sim 1/(\omega_c W)^2$.

In Fig. S7 we schematically plot the dependencies $I(\omega_c)$ and $\varrho_{xx}(\omega_c)$ near and far from the transition ballistic-hydrodynamic and the ballistic-Ohmic transitions. At $0 < \omega_c W - 2 \ll 1$ these curves are described by Eq. (S91) and (S97). At $\omega_c \gg 1/W$ they follow asymptotes (S99) and (S100).

4. COMPARISON WITH PRECEDING THEORETICAL AND EXPERIMENTAL WORKS

4.1. Related theoretical works

In Ref. [25] a numerical solution of the kinetic equation (S2) is carried out for the same system as we study in this work: a long narrow sample with rough edges. The kink in the dependencies of the resistances ϱ_{xx} and ϱ_{xy} on magnetic field B at the transition point $B = B_c$ was also obtained. Although the authors of Ref. [25] discussed the emergence of the central electrons above the transition those do not scatter on the edges, the electron

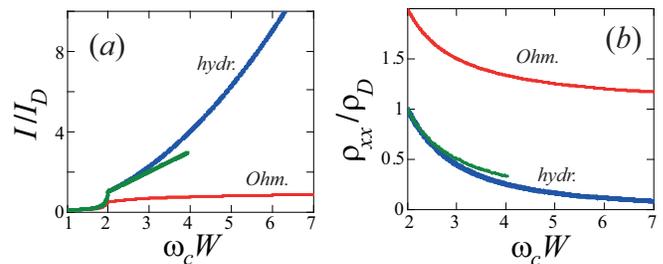


FIG. S7: Current (a) and longitudinal resistance (b) as functions of magnetic field near and far beyond the critical field $\omega_c = 2/W$ for the ballistic-hydrodynamic and the ballistic-Ohmic phase transitions. The curves for the Ohmic samples are plotted by exact formulas (S97). The green curves for I and ϱ_{xx} in the vicinity of the ballistic-hydrodynamic phase transition are drawn by formula (S91), which does not take into account the inhomogeneous distribution of central electrons. The asymptote of all curves at $\omega_c \gg 1/W$ correspond to Eqs. (S100) and (S99).

dynamics just below the transition, $B < B_c$, and the interaction between the edge and the central electrons above the transition, $B = B_c$, were not considered. The dependencies $\varrho_{xx}(B)$ and $\varrho_{xy}(B)$ obtained in the current work by analytical calculations (Fig. 3 in the main text) are very similar to the ones obtained in Ref. [25] for the narrow samples, $W \ll 1/\gamma$ [Fig.1 (a) and Fig.1 (a) in that Letter].

In Ref. [26] the ballistic transport of 2D electrons in a long stripe was theoretically examined in details. Similar general formulas for the distribution function in the ballistic regime [see Eq. (S20)] and for the simplified distribution function in the second ballistic subregime [see Eq. (S28)] as well as the numeric description of the transport regime at $\omega_c W - 2 \sim 1$ were obtained.

In the present paper we have further developed the studies of the ballistic and the hydrodynamic electron transport as compared with the results of Ref. [26]. Namely, in the current work we have provided the description of the flow in the first and the third ballistic subregimes; explained the origin of the bulk contribution to the Hall resistance $\varrho_{xy} = \varrho_{xy}^0/2$ in the limit $B \rightarrow 0$; as well as revealed and studied the ballistic-hydrodynamic and the ballistic-Ohmic phase transitions.

4.2. Related experiments

In this subsection we briefly discuss experiments [8], [9], and [17], in which the ballistic-hydrodynamic transition was apparently observed.

In Ref. [8] a Poiseuille flow of a 2D electron fluid in a graphene stripe was experimentally studied. Magnetoresistance and the distribution of the Hall field over the cross section of the stripe were measured in a wide range of magnetic fields and electron densities. The experimen-

tal dependence $\varrho_{xx}(B)$ is very similar to the theoretical one on Fig. 3(a) in the main text. It exhibits a non-monotonous behavior at $B < B_c$, a smeared kink at the transition field $B = B_c$, and a monotonous decrease at $B > B_c$. In the vicinity of $B = 0$ the positive magnetoresistance corresponding to the importance of the contribution from the skipping electrons is observed. Thus, the ballistic dynamics and ballistic-hydrodynamic phase transition revealed in our work was apparently realized in experiment [8]

In Ref. [9] a direct observation of the profile of the current density $j(y)$ for a Poiseuille flow in a graphene stripe was performed by measurements of the local magnetic field induced by the distribution of $j(y)$. Additionally, magnetoresistance of the graphene stripe being very similar to the magnetoresistance reported Ref. [8] was observed (see Fig. 21 in Supplemental Information of Ref. [9]). In particular, a maximum at $\omega_c W \sim 1$ and a sharp kink at $\omega_c W = 2$ in the dependence $\varrho_{xx}(\omega_c)$ were clearly observed in Ref. [9].

In Ref. [8] the Hall field profiles $E_H(y)$ were measured in the central part of the stripe. In the ballistic regime these profiles turned out to be nearly flat, while in the hydrodynamic regimes they were strongly curved, similarly to the parabolic hydrodynamic profiles corresponding to the Poiseuille flow). We believe that the sharp features in $E_H(y)$ near the sample edges, $y = \pm W/2$, predicted in our theory for the all ballistic subregimes [see Fig. S4 and Fig. 2 in the main text] can be observed in experiments similar to one of Ref. [8], provided the profiles $E_H(y)$ will be measured up to the sample edges.

In Ref. [18], a Poiseuille flow formed by 2D electrons in a long sample of high-mobility GaAs quantum wells was observed. The dependence of the resistances ϱ_{xx} and ϱ_{xy} on magnetic field B were measured. Apparently, the system studied in Ref. [18] was close to the ballistic transport regime at $W < 2R_c$ and to the hydrodynamic regime at $W > 2R_c$. The experimental dependence $\varrho_{xx}(B)$ is rather similar to the theoretical one in Fig. 3(a) in the main text. The experimental result for $\varrho_{xy}(B)$ is also rather similar to the theoretical one obtained in the current work [see Fig. 3(b) in the main text]: it exhibits positive and negative deviations from the standard Hall resistance $\varrho_{xy}^{(0)} = B/(nec)$ below the transition point, $W < 2R_c$, and an almost exact coincidence with $\varrho_{xy}^{(0)}$ above the transition point, $W > 2R_c$. However, the signs of the deviation of ϱ_{xy} from $\varrho_{xy}^{(0)}$ in the vicinity of $B = 0$ and near $B = B_c$, as we understood from Ref. [18], are opposite to the signs in our theoretical

result [see Fig. 3(a) in the main text]. Perhaps this discrepancy is associated with a different definition of the sign of ϱ_{xy} and $\varrho_{xy}^{(0)}$ in our work and Ref. [18].

So the predicted magnetic field dependencies of the longitudinal and, possibly, of the Hall resistances in the ballistic regime as well as around the ballistic-hydrodynamic phase transition were observed in Refs. [8], [9], and [18].

Additionally, we note that the negative ballistic magnetoresistance (S47), corresponding to the bulk contribution from the ballistic trajectories between the sample edges [the small peak near $B = 0$ in Fig. 3(a)], was apparently observed in high-mobility GaAs quantum wells containing macroscopic oval defects in experiments [11–13] (for a detailed discussion see Refs. [28, 29]).

Indeed, the analysis in Ref. [19] of the magnetotransport experiments on the GaAs quantum wells analogous to the ones studied in Refs. [11–13] demonstrates that the geometry of the 2D electron flow in that experiments is different from the Poiseuille flow. Due to the presence of the macroscopic oval defects inside the samples, the effective width W_{eff} of the flow is apparently estimated as the mean distance between the macroscopic defects. Therefore the ballistic regime is realized when the mean free path l and the cyclotron diameter $2R_c$ are larger than the effective channel width W_{eff} , but not than the actual sample width $W > W_{eff}$.

Such flow geometry with irregular channel edges may lead to the domination of the bulk contribution in magnetoresistance (from the trajectories between the opposite channel edges) in the first ballistic subregime, $\omega_c \ll \gamma^2 W_{eff}$, unlike the case of long stripes with straight edges studied in Refs. [8], [9], and [18], where the contribution of the skipping electrons to magnetoresistance apparently dominates in analogous subregime, $\omega_c \ll \gamma^2 W$. Correspondingly, the negative bulk ballistic magnetoresistance (S47), corresponding to the suppression of the edge positive magnetoresistance (S56) by the edges roughnesses, was possibly observed in experiments [11–13].

Finally, we note that the sharp ballistic-hydrodynamic phase transition may be realized not even in stripes of 2D high-mobility conductors, but in a much wider class of systems, in particular, in the just discussed high-mobility GaAs quantum wells with rare (see Ref. [15] for experimental report about such systems and Refs. [19],[28] for discussion of realization of the hydrodynamic and the ballistic regimes of transport in them).